5 Mapping glacial lineaments from satellite imagery: an assessment of the problems and development of best procedure

5.1 Introduction

The ability to detect and map landforms on satellite imagery is comprised of two elements:

- the mapping ability and specialist experience of the observer.
- the spectral and physical characteristics of the sensor and their interaction with the imaged surface.

The first element has been shown in limited scenarios to be highly variable *between* different observers. Although this variability can never be entirely removed, it can be mitigated against by well defined and meticulous mapping procedures. It is the former element that this chapter now addresses, providing an assessment of problems through a series of experiments using multiple images of a series of test areas, and a Digital Elevation Model (DEM). A procedure for best practice is then developed. The impetus for this research came from initial glacial landform mapping in Ireland using radar imagery and a review of this work is provided as an example of the problems in landform detectability.

The representation of a landform on an image is controlled by the size of the landform in relation to the resolution of the image (*relative size*), the orientation of the landform with respect to the incident solar illumination azimuth (*azimuth biasing*) and the tonal and textural definition of the landform on an image (*landform signal strength*). These three variables interact, producing a complex "surface" of landform representation. That is, they each effect landform representation in different ways in different parts of the image. This chapter attempts to highlight the propagation of these biases and provide guidelines for

minimising their effects. An earlier version of this work has been published (Smith *et al*, 2001).

5.2 Methodology

In order to assess the impact of the above variables on landform representation, suitable images from a range of earth resources satellites are required. A study area that contained enough lineaments to be statistically viable needed to be selected. The region around Lough Gara, County Roscommon, Ireland (1539km^2), bounded by the Ox Mountains on the west and the town of Sligo to the north, was selected (Figure 5.1). There is complete coverage from four of the five main earth resources sensors; Landsat MSS, Landsat TM, SPOT Panchromatic and ERS-1 Synthetic Aperture Radar (SAR). Unfortunately there were no suitable cloud free scenes for Landsat ETM+ available for this study area, so a second test area on the Kola Peninsula (1183km^2), Russia, has been used to supplement the results.

The above images, and the lineaments mapped from them, are initially visually assessed through descriptive inter-image comparisons (§5.3.1). They are then analysed through the experimentation described in §5.2.3.

Given the differences between the SAR and VIR sensors a case study (§5.4) is used to illustrate the complementary nature of SAR imagery, in addition to the inter-image comparisons. The SAR case study area (2150km^2) lies west of Strangford Lough, County Down, Ireland, bordered on the south by Dundrum Bay (Figure 5.1). A discussion of inter-image comparisons from the Lough Gara region (§5.5) is also presented, providing a case study showing the effects of representation biases in this area.

The chapter concludes with a summary of the results and the main issues resulting from them. Recommendations for the most appropriate satellite imagery to acquire in order to map glacial lineaments, with respect to relative size, azimuth biasing and landform signal strength, are presented. This includes a discussion about calculating the most appropriate dates for image acquisition.

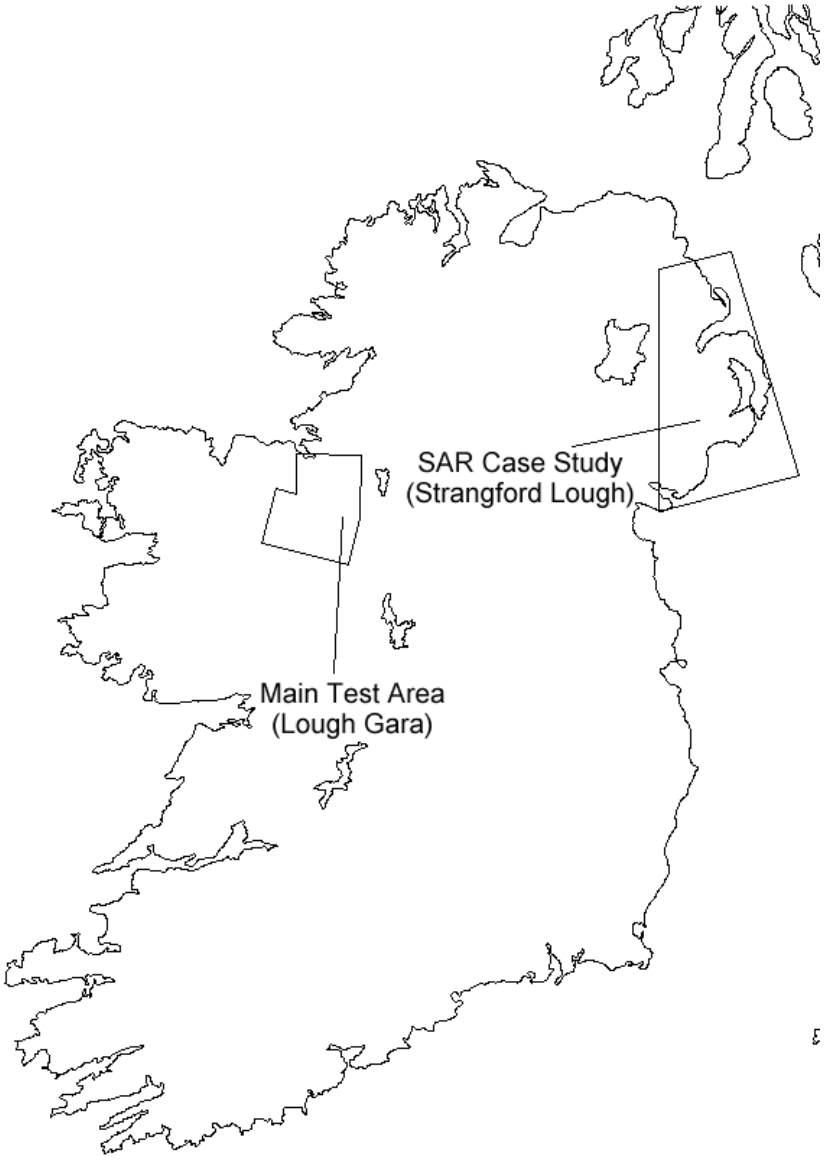

Figure 5.1 Location of the main test area (Lough Gara) and SAR case study area (Strangford Lough) in Ireland.

5.2.1 Accuracy Assessment

Appendix 3 broadly discusses spatial data accuracy with reference to the different elements of accuracy, the general schemes used to assess accuracy and methods to mitigate against error. In order to assess the accuracy with which landforms can be mapped from each type of imagery it is necessary to have good information on the landforms which are known to be present in the test area. However, as it is not possible to completely know which landforms are actually present, accuracy assessment can only be accomplished by comparison with the most accurate measurement available (i.e. "truth").

For this purpose a high resolution DEM (Figure 5.2a) was used to create a morphological map (now simply referred to as *truth*) for a subset of the area (587km^2). Computer aided relief shading is an effective method for visualising a DEM and mapping landforms (see §5.2.2). This suffers from the same azimuth biasing as satellite imagery. Therefore the morphological map was produced through full break-of-slope mapping using multiple illumination azimuths (Figure 5.2). A comparison of truth with a selection of the original stereoscopic aerial photography and topographic mapping confirmed its accuracy.

The DEM was created by the Irish Ordnance Survey from 1:40000 stereoscopic aerial photography at a spatial resolution of 50m, using a digital analytical plotter (O'Reilly, pers. comm 2003). The spatial resolution of the DEM is similar to that of the imagery, but because the landform mapping is based upon stereoscopy rather than photo interpretation, and because the original photographs are at a higher resolution than the satellite imagery, the morphological map produced from the DEM will be at a higher level of accuracy than is possible using satellite imagery.

In addition, relief shading (§5.2.2) assumes an homogenous, specular, surface. The relief shaded scene therefore visualises high reflectance from all surfaces. Although this does not accurately simulate the diversity of real world surface reflectance, it has the effect of highlighting subtle topographic variations.

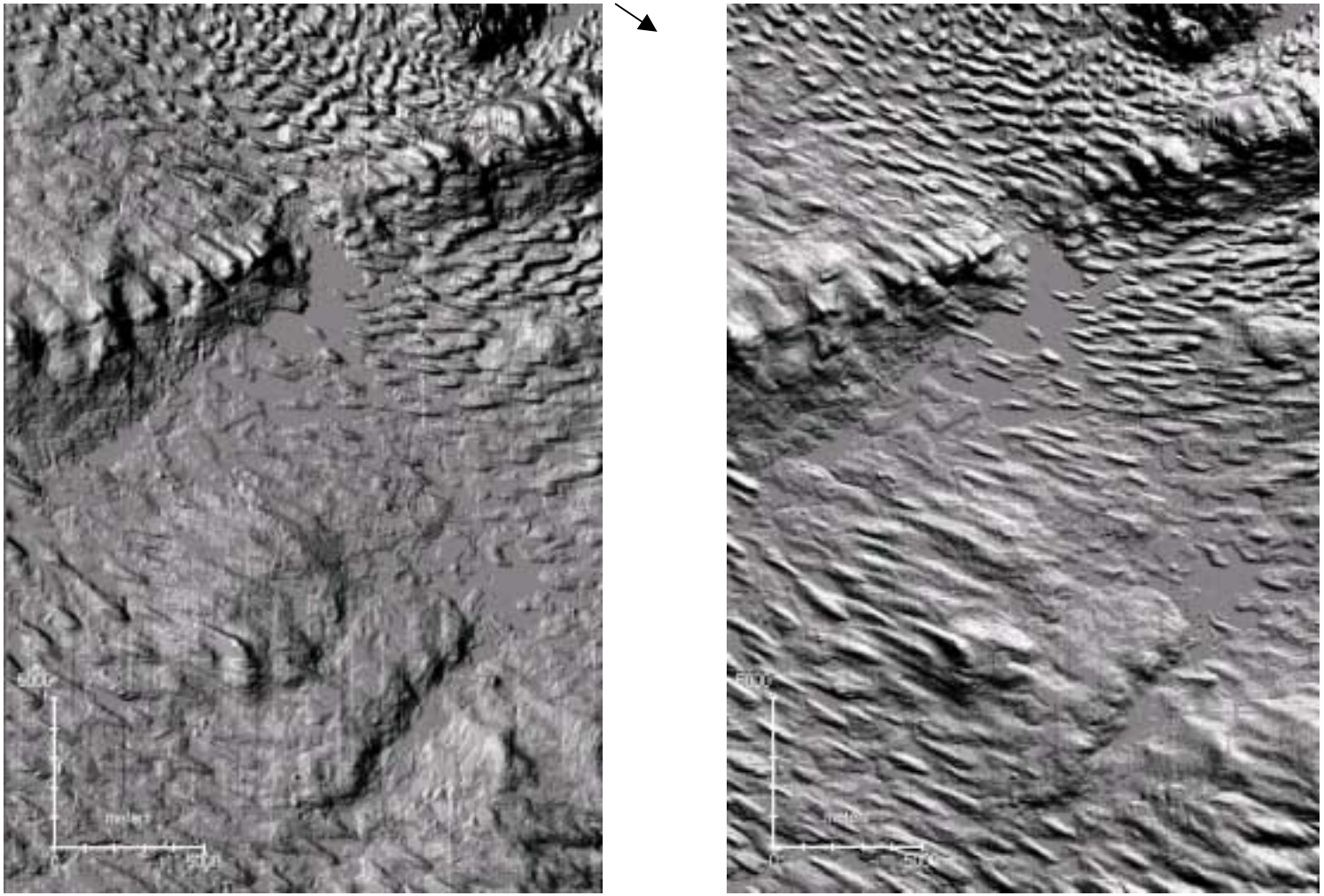

Figure 5.2a and b Hillshaded DEM of Lough Gara, Ireland, using an illumination azimuth parallel (left) and orthogonal (right) to the principal lineament orientation. Note the dramatic changes in lineament morphology, particularly above the centre of the image. Arrows indicate the azimuth angle.

5.2.2 Computer Rendering Techniques

Computer rendering is the graphical recreation of a real word scene through numerical modelling and visualisation on a computer monitor. There are a number of techniques used to perform rendering, either predominantly physically or visually based. Relief shading by fixed azimuth (i.e. solar illumination) is one of several computer rendering techniques that is commonly used within 3D visualisation environments, including GIS (e.g. Figure 5.2). Generally, it is less effective than other methods at producing realistic images (see Appendix 1), however it is fast and efficient, making it suitable for many environmental science applications. Other rendering techniques were explored (e.g. ray shading), however these results were not satisfactory and so were not pursued any further. Appendix 1 provides a brief introduction to the main rendering techniques currently employed.

5.2.3 Orientation Data

Within geology and geomorphology, orientation data are used extensively to refer to attributes of spatial phenomena (e.g. lineaments, faults). These are usually recorded as compass bearings relative to north and can be analysed and visually presented in a number of ways. For example, rose diagrams and Corona plots can be used to display orientation data. However, fundamental to orientation data is that 0°=360° and therefore many standard statistical summaries are not appropriate (e.g. the mean of 1° and 359° cannot be 180°). An appropriate approach to analysing orientation data is to treat them as vectors (Cox, 2001). If the phenomena are recorded simply as an orientation then, each vector can be given unit weight. However other orientation data may well have a magnitude that can be applied as well (e.g. wind speed and direction). This chapter is concerned with lineaments of a certain orientation and so the former case is applicable. It is therefore appropriate to calculate the vector mean as:

$$S = \sum \sin q$$

$$C = \sum \cos q$$

$$\bar{q} = \arctan(S / C)$$

where *?* is the orientation (in degrees) and $\bar{q}$ is the vector mean. The strength ('parallelness') of the resultant vector (mean resultant length) can be calculated as:

$$\bar{R} = \sqrt{S^2 + C^2} / n$$

where *n* is the number of observations. $\bar{R}$ varies between 0 and 1, with 1 representing orientation in the same direction and 0 in multiple directions. The latter can occur from a variety of situations, such as a uniform distribution or evenly distributed clusters. Vector strength can also be used as a surrogate for the standard deviation. Chapters 5, 6 and 7 discuss orientation of lineaments in detail and therefore analysis using vectors is used extensively.

5.2.4 Experiments

1) **Landform Signal Strength** – In order to assess the effect of varying solar elevations on landform representation, imagery would have ideally been obtained from the same sensor over a range of solar elevation angles. The difficulty in obtaining cloud free scenes, and because the azimuth angle also varies with elevation angle meant that this was not practical. Therefore a visual comparison was performed between two images broadly categorised as having low and high solar elevation angles.

It was also hoped to use a DEM to model the effects of landform signal strength by simulating different solar elevations through the use of relief shading, however the results were not satisfactory (see Appendix 1) and, after pursuing alternative rendering techniques (see §5.2.2), this line of inquiry was dropped.

2) **Azimuth Biasing Effect** – In order to assess the biasing effect, an image with a single illumination azimuth but varying lineament orientations was used. A relative comparison was then performed between the image and truth.

A further experiment was also performed using the DEM to investigate azimuth biasing more objectively by simulating different azimuth angles through the use of relief shading. All lineaments were mapped and then compared with truth.

3) **Relative size** – In order to assess the effect of image spatial resolution on landform representation a Landsat ETM+ image was obtained, which is ideally suited to this task, as the high resolution panchromatic band (15m) and lower resolution multispectral bands (30m) are acquired at the same time and hence solar illumination is the same. Band 2 was selected to compare against the Panchromatic band, as a greyscale image was appropriate and they both record an overlapping part of the EM spectrum.

SPOT Panchromatic, Landsat TM Band 5 and Landsat MSS Band 4 were used for all lineament mapping (Table 5.1). The Landsat TM and MSS bands were chosen as the near-IR enhances any moisture variations (Clark, 1997), whilst tonal variations are more efficiently detected by the human eye from a greyscale image (Estes *et al*, 1983). Where appropriate all images had pre-processing techniques applied to them following the guidelines of Clark (1997). All mapping was performed by one observer and observer variability is assumed to be minimal through consistency produced by this.

Satellite Images	**Spatial Resolution (m)**	**Date**	**Lat/Long (°) of Image Centre**	**Illum Elev (°)**	**Illum Az (°)**
Lough Gara					
ERS-1 SAR	25	04/08/92	54:14N 8:53W	23.1	104D
ERS-1 SAR	25	02/03/93	54:19N 8:51W	23.1	104D
Landsat TM	30	10/12/	53:39N 7:43W	11.2	160
Landsat TM	30	06/05/89	54:51N 7:58W	48.3	147
Landsat MSS	80	06/01/83	54:51N 7:45W	10.1	157
SPOT Panchromatic	10	28/11/92	53:39N 8:20W	14.3	167
SPOT Panchromatic	10	28/11/92	54:07N 8:10W	13.9	168
Strangford Lough					
ERS-1 SAR Landsat TM	25 30	30/06/93 03/11/90	54:28N 6:00W 54:31N 4:28W	23.1 18.1	256A 158
Kola Peninsula					
Landsat ETM+	15/30	17/07/99	66:57N 32:24E	43.8	166

Table 5.1 Meta-data for satellite imagery used in this study (D=descending, A=Ascending).

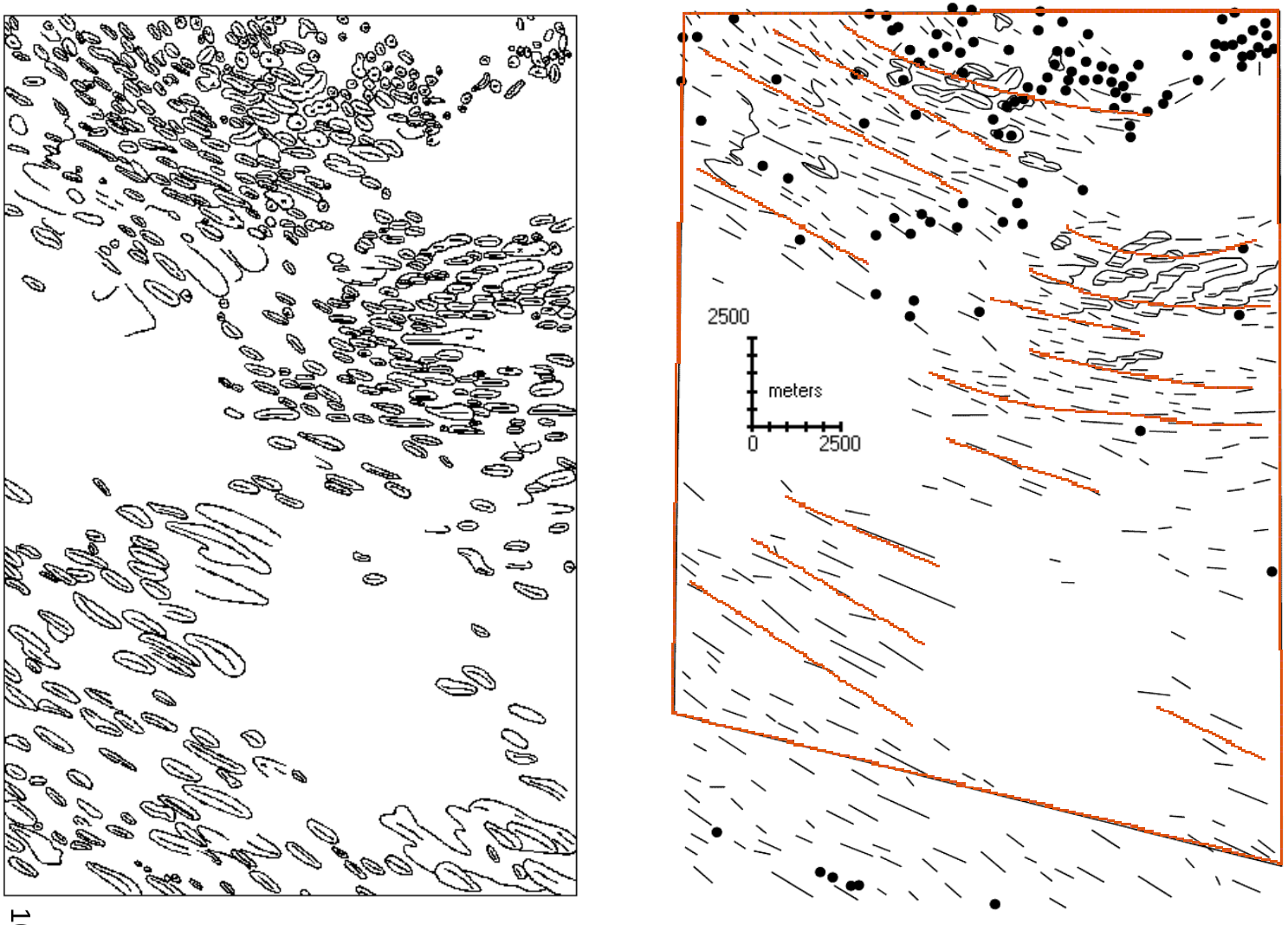

Figure 5.3 (a) Morphological map (truth) created from a high resolution DEM using break-of-slope mapping for Lough Gara, Ireland. (b) Data from (a) were then generalised. Lines represent lineaments, points represent hillocks and polygons represent transverse ridges. The box outline shows the area of overlap with the satellite imagery. The red outlined overlay shows generalised flow patterns.

5.3 Results

These sections present the results of inter-image comparisons and analysis of the controls on detectability. The first section provides a description both of the images and of the landforms mapped from them, whilst the second section presents summary statistics for each experiment. The figures are further illustrated with zoomed sections of the Landsat MSS, Landsat TM, SPOT and SAR images.

5.3.1 Inter-image Comparisons

Truth

Figure 5.3b shows a map of all detectable lineaments produced from truth (Figure 5.3a) for a subset of the Lough Gara study area (this is outlined on all subsequent satellite images). There is a strong trend of lineaments oriented NW-SE, with longer lineaments in the southern area. A spread of lineaments oriented E-W is also noticeable. There is a strong concentration of hummocky terrain in the northerly part of the map, with few hummocky forms elsewhere.

The northern half of the map also contains transverse ridges, often with lineaments overlying them. This map is taken to be the most accurate representation of the landforms present (i.e. “truth”) against which the other images are tested.

Landsat MSS Image

The low contrast and spatial resolution (80m) within the image leads to poor lineament detection (Figure 5.4b and zoomed section in Figure 5.5). Although the southern portion of the image depicts E-W trending lineaments, curving to the NE, this is not clear and is barely detectable in many parts. The presence of hummocky terrain in the central portion is clearer, whilst the northern area depicts clearly detectable lineaments although their trend is not so obvious. The forms in the south, whilst less detectable, appear wider and longer. The overall impression is one of an ability to see lineaments, but not identify and map them precisely.

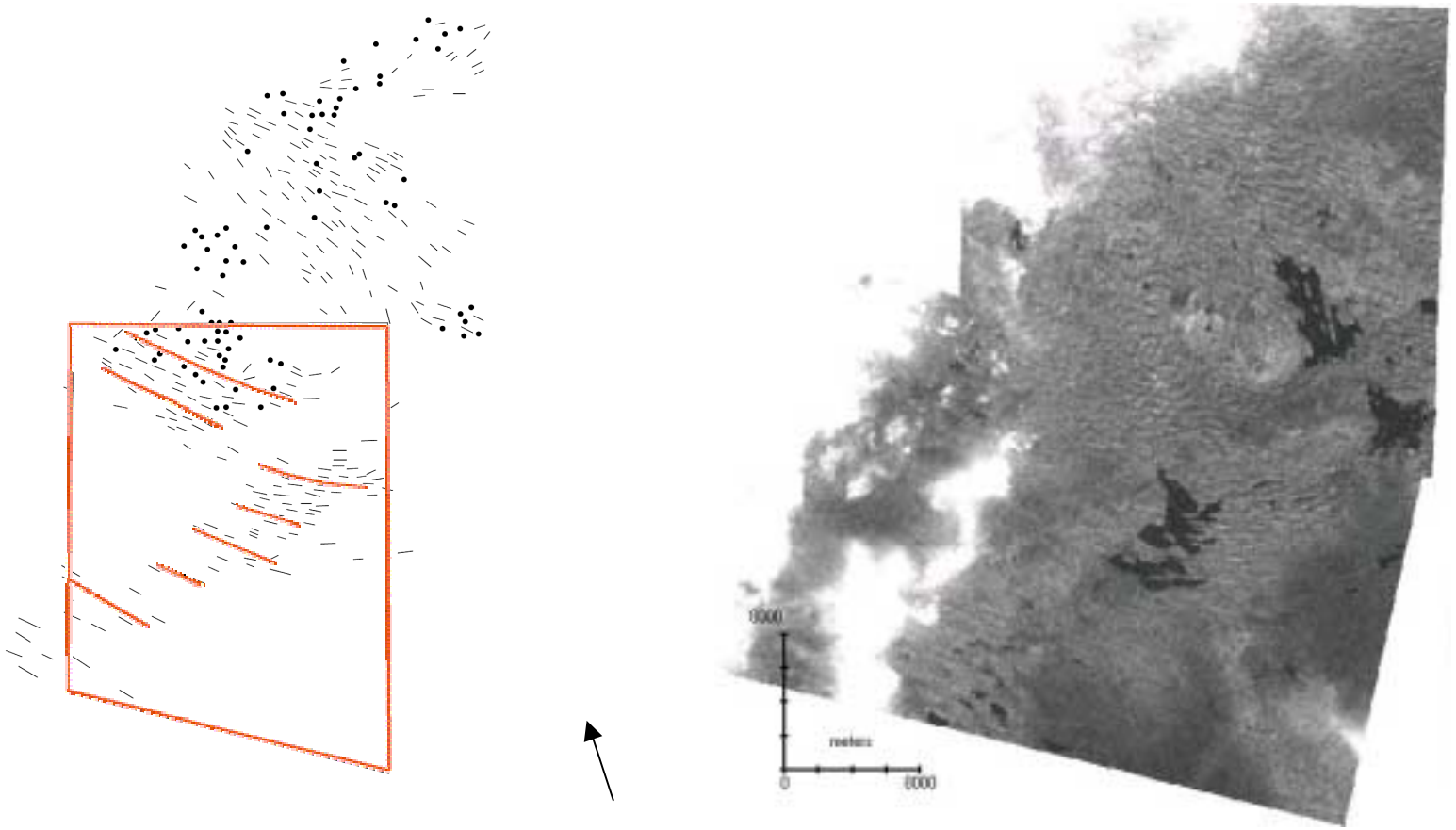

Figure 5.4a and b Landsat MSS glacial lineament map (left) and image (right) for Lough Gara, Ireland. Arrow indicates azimuth angle. The red outlined overlay shows generalised flow patterns.

Figure 5.5 Zoomed portion of the Landsat MSS image for Lough Gara.

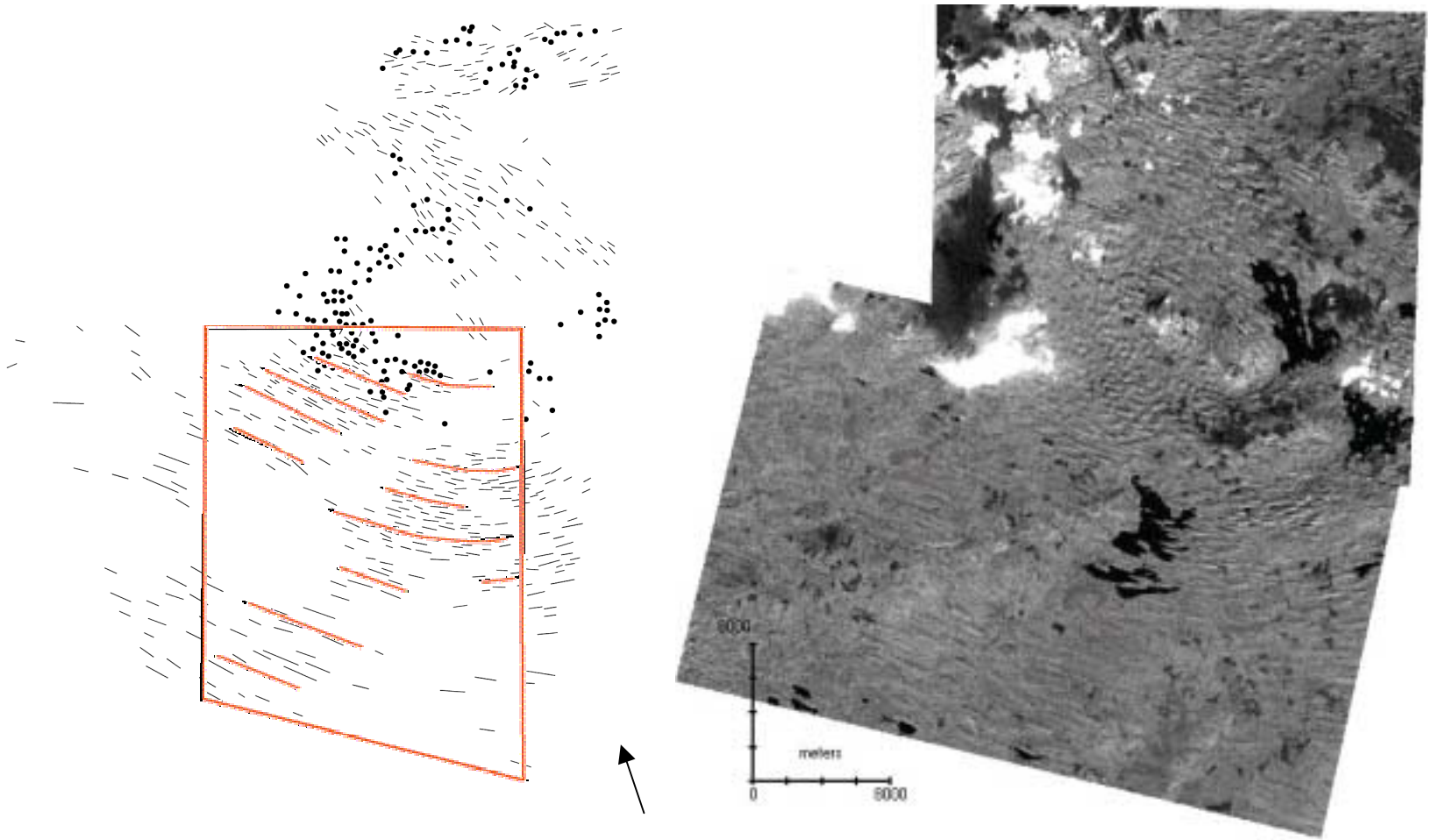

Figure 5.6a and b Landsat TM glacial lineament map (left) and image (right) for Lough Gara, Ireland. Arrow indicates azimuth angle. The red outlined overlay shows generalised flow patterns.

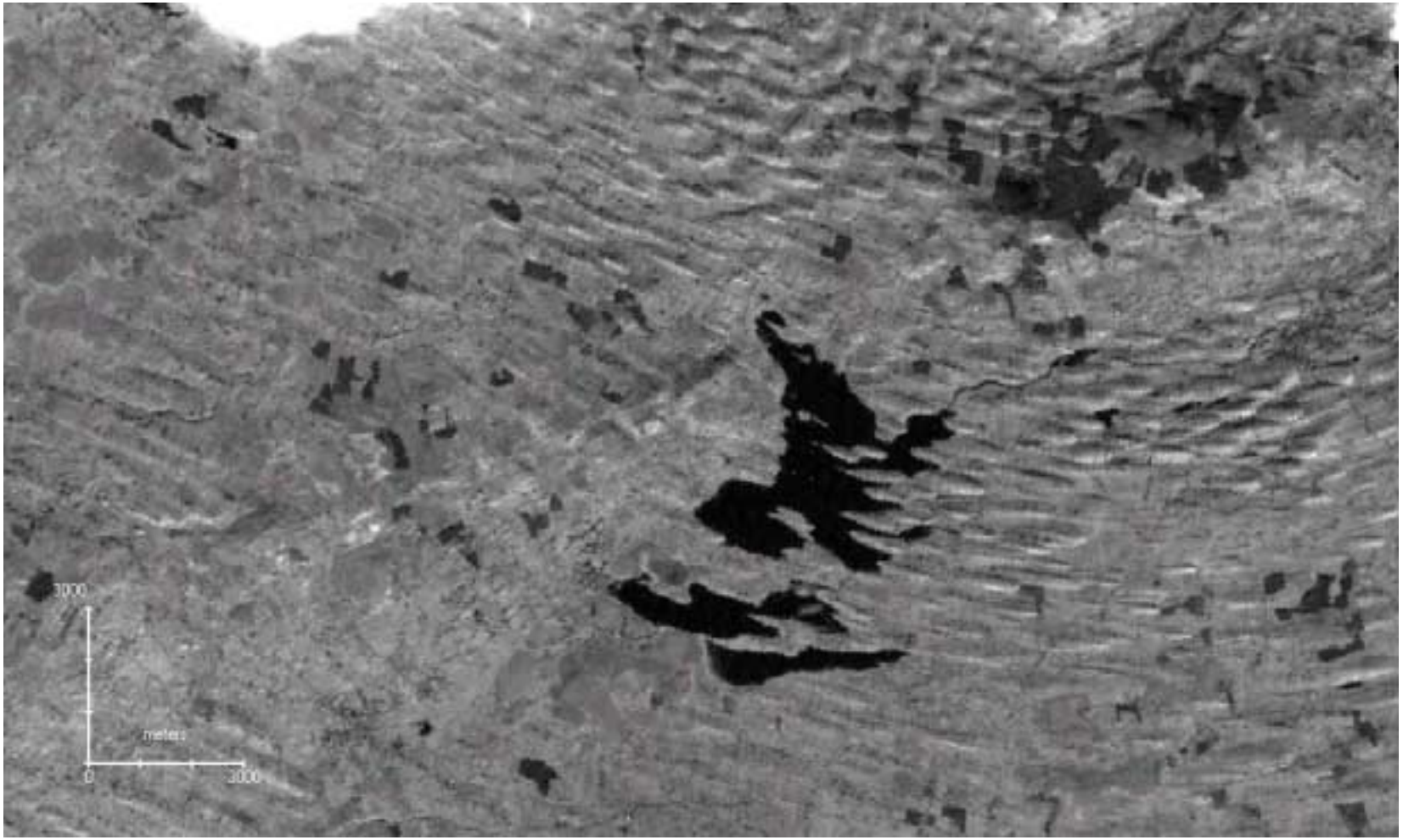

Figure 5.7 Zoomed portion of the Landsat TM image for Lough Gara.

Figure 5.4a shows the lineaments that have been mapped from this image. There is a strong lineament orientation of NW-SE, with some lineaments in the east trending W-E and some in the north trending SW-NE. The central area has a greater abundance of hummocky terrain, with further hummocks in the northern area. In general there are far fewer lineaments mapped in comparison to truth, however the main trends are readily apparent, although no transverse ridges have been identified.

Landsat TM Image

The topographic shadows increase the amount of contrast present, which, in addition to the increase in spatial resolution (30m), in comparison to Landsat MSS, produces a high quality image (Figure 5.6b and zoomed section in Figure 5.7) allowing the straightforward recognition of landforms.

In the southern portion of the image long, broad lineaments are visible in the west (trending east-west), becoming more apparent in the east whilst curving towards the NE. The central region shows hummocky terrain, comprised of many small circular hills. In the northern part of the image there is a clear orientation NW-SE, although in the extreme NE corner lineaments are again trending E-W.

In contrast to the MSS mapped data, Figure 5.6a shows a greater number of lineaments mapped, although still less than for truth. The same general pattern is visible between all three maps. In comparison to the MSS mapped data, the eastern area shows a clear transition in lineament orientation from NW-SE to NE-SW. In addition, the northern area shows some lineaments cross-cutting one another.

SPOT Panchromatic Image

Simple contrast enhancements were necessary in order to make the best use of this high resolution (nominal 10m pixel size) image (Figure 5.8b and zoomed section in Figure 5.9). Initial assessment of the amount of contrast available for lineament mapping suggests a high quality image, although closer inspection reveals that the contrasts are more subdued and, although landforms are

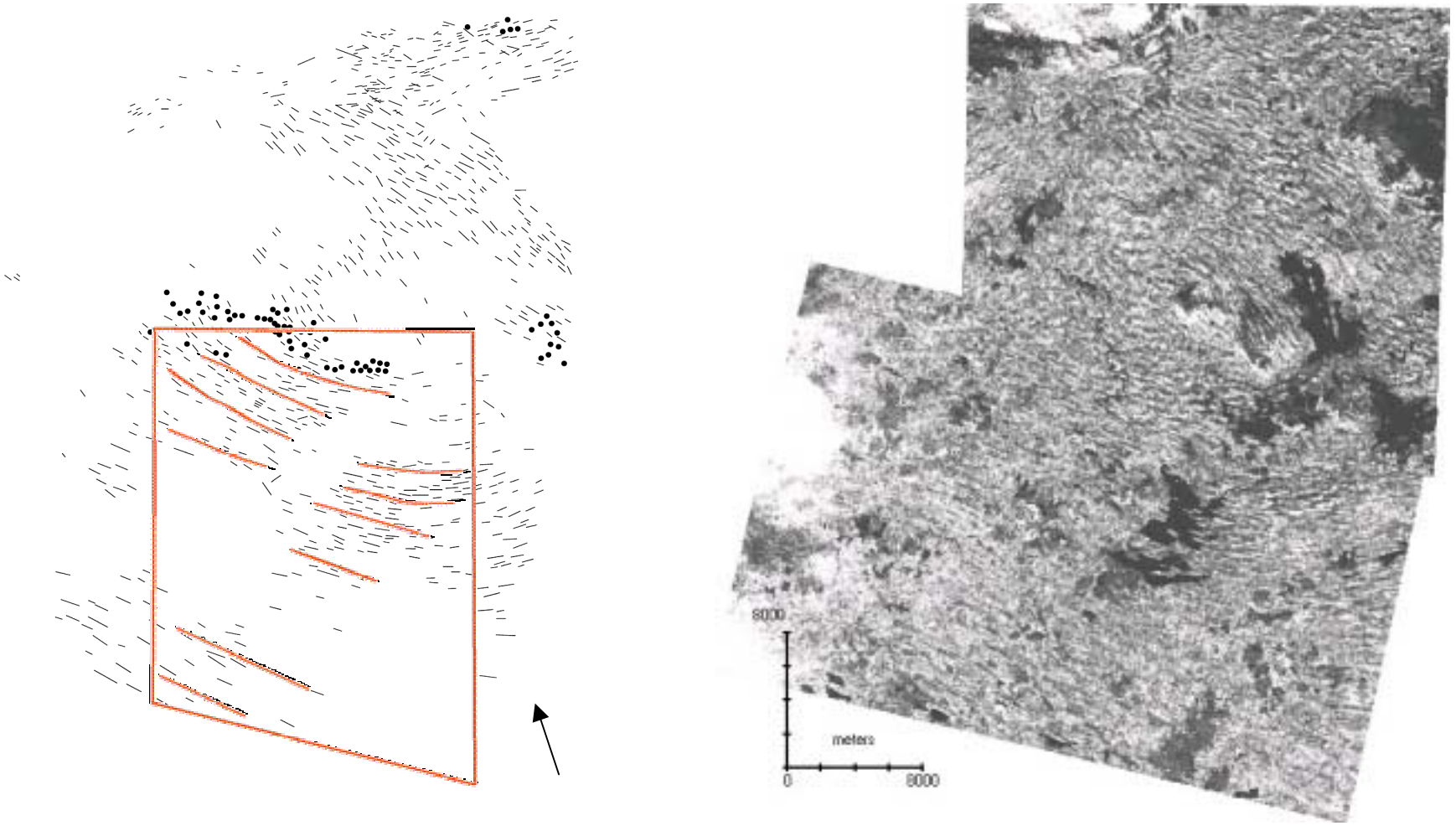

Figure 5.8a and b SPOT glacial lineament map (left) and image (right) for Lough Gara, Ireland. Arrow indicates azimuth angle. The red outlined overlay shows generalised flow patterns.

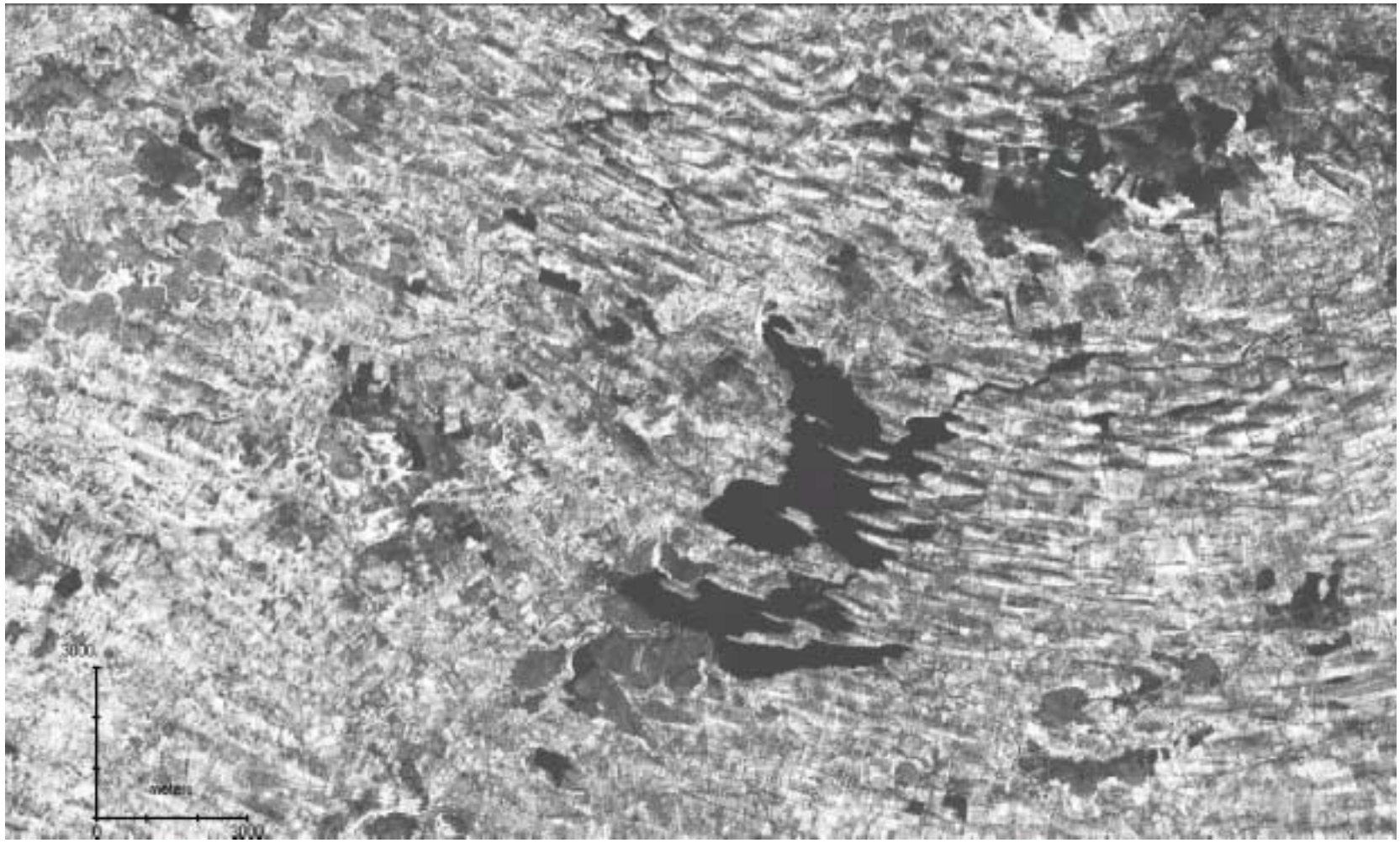

Figure 5.9 Zoomed portion of the SPOT image for Lough Gara.

clearly visible, their representation is not as good as with the TM image. However the high spatial resolution allows detailed landform mapping, clearly showing areas of intersection between E-W and NW-SE trending lineaments in the northern region. The southern region shows longer lineaments in the W trending NW-SE, curving towards NE-SW in the eastern area. The central region appears as a more complicated area of “hummocky” terrain, with elongate and ovoid forms present. Like the truth, TM and MSS mapped data, the SPOT data again shows the same general trends (Figure 5.8a). There are even more lineaments mapped than in any of the previous images (Table 5.2), although less than the truth. There are noticeably fewer hummocks than the Landsat MSS and TM images and a greater incidence of crossing lineaments in the northern portion of the image.

ERS-1 SAR Image

The SAR image (Figure 5.10b) is initially very striking simply because it is visually different from the other VIR imagery (zoomed section in Figure 5.11). Close inspection, and familiarity with working with SAR imagery, shows the presence of NW-SE oriented lineaments in the northern region. In the NE corner there are also lineaments oriented NE-SW. The northern western area also has several lineaments oriented NE-SW. This area grades into hummocky terrain in the central region. In comparison to the VIR imagery, Lough Gara is difficult to locate and, once found, there are very few lineaments visible. Indeed the whole of the southern portion of the image shows very few lineaments.

This inspection is born out by the lineament mapping (Figure 5.10a), generally showing far fewer lineaments mapped than in any other image with almost a complete absence of the central area of curving flow. However the lineaments oriented on the eastern and western sides of the north of the image are better defined and more numerous than on the VIR imagery.

Landsat ETM+ Image

Panchromatic

Simple contrast enhancements were again employed to prepare the image. The high contrast within the image is mainly manifested through spectral

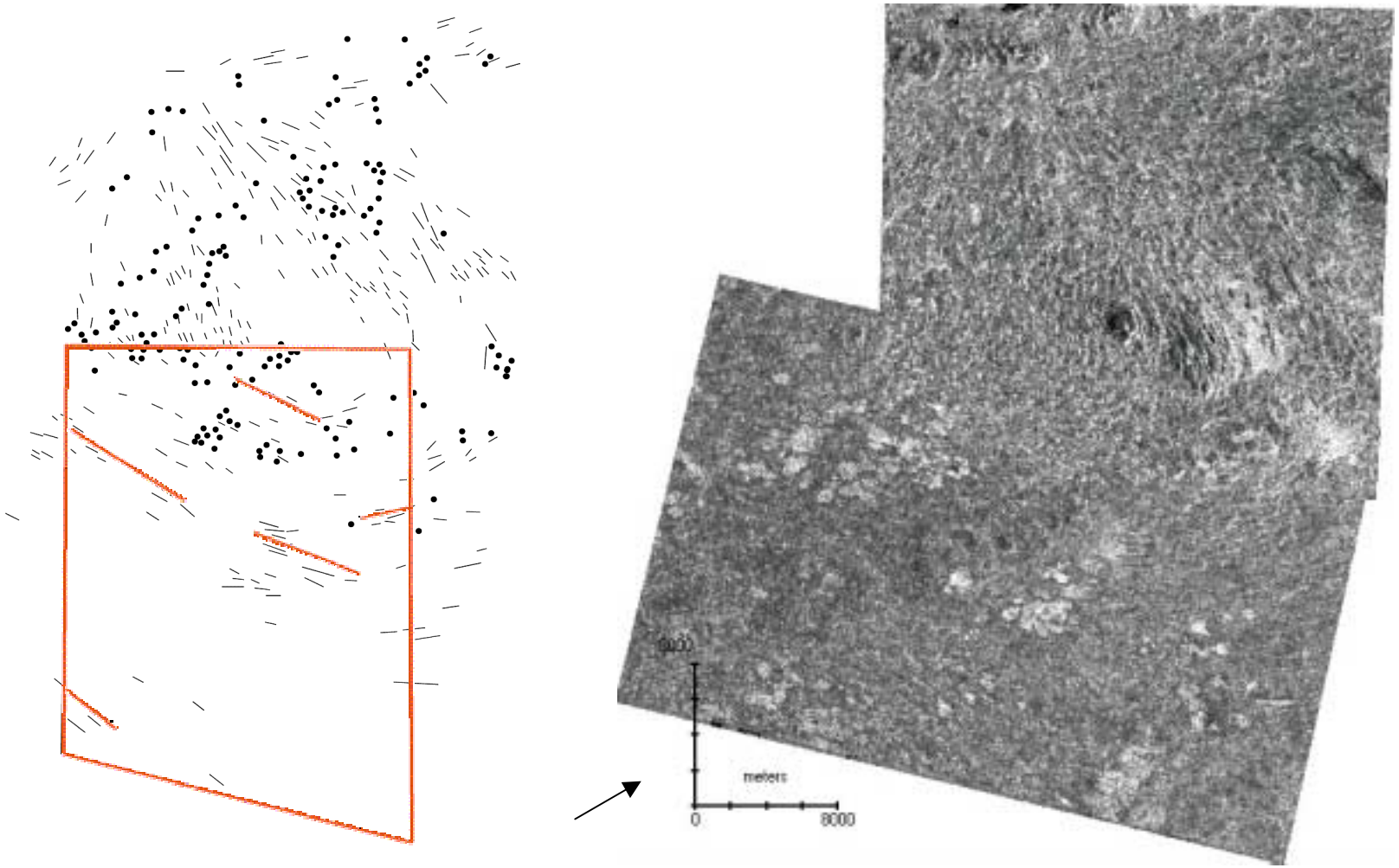

Figure 5.10a and b ERS-1 SAR glacial lineament map (left) and image (right) for Lough Gara, Ireland. Arrow indicates azimuth angle. The red outlined overlay shows generalised flow patterns.

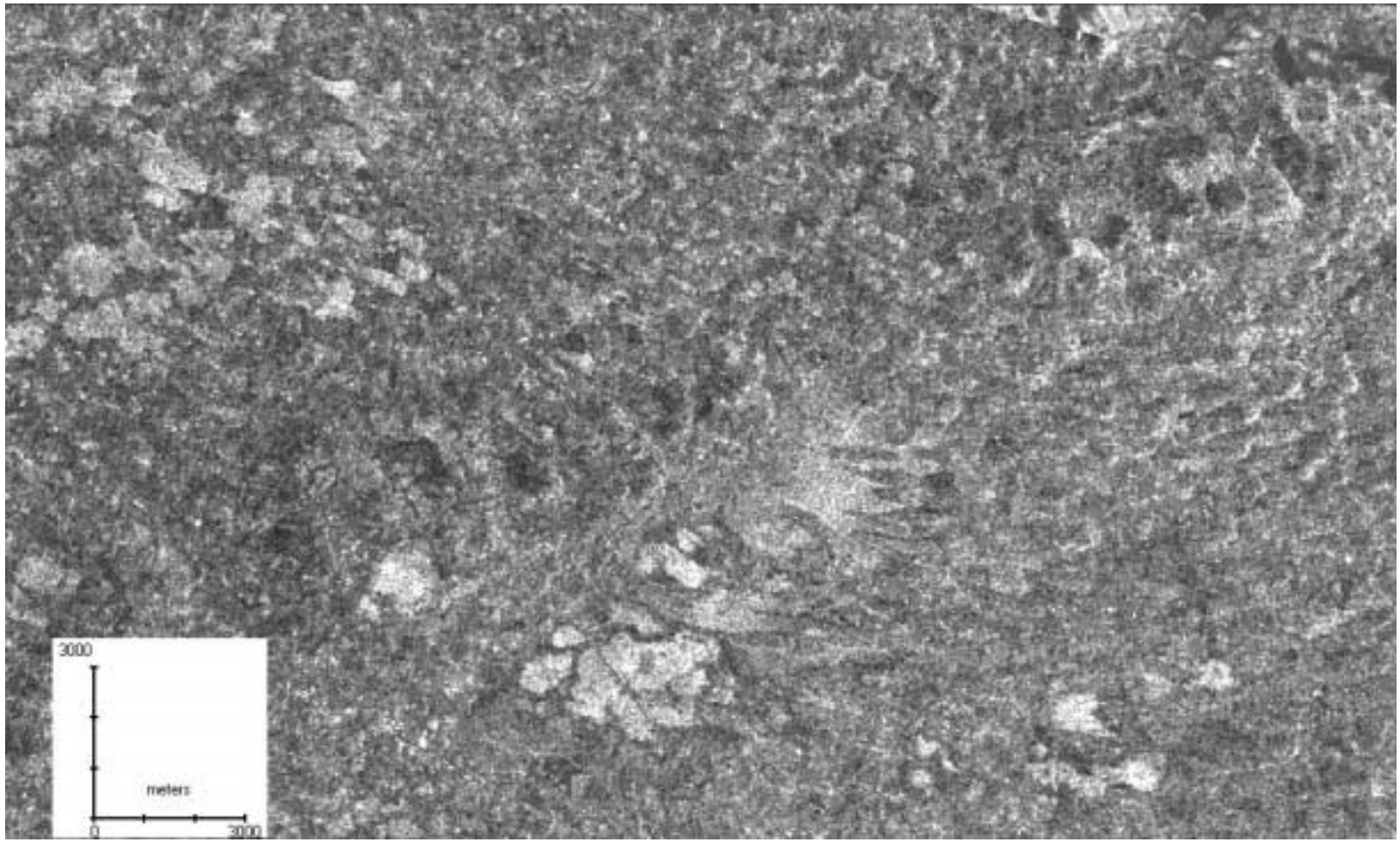

Figure 5.11 Zoomed portion of the ERS-1 SAR image for Lough Gara.

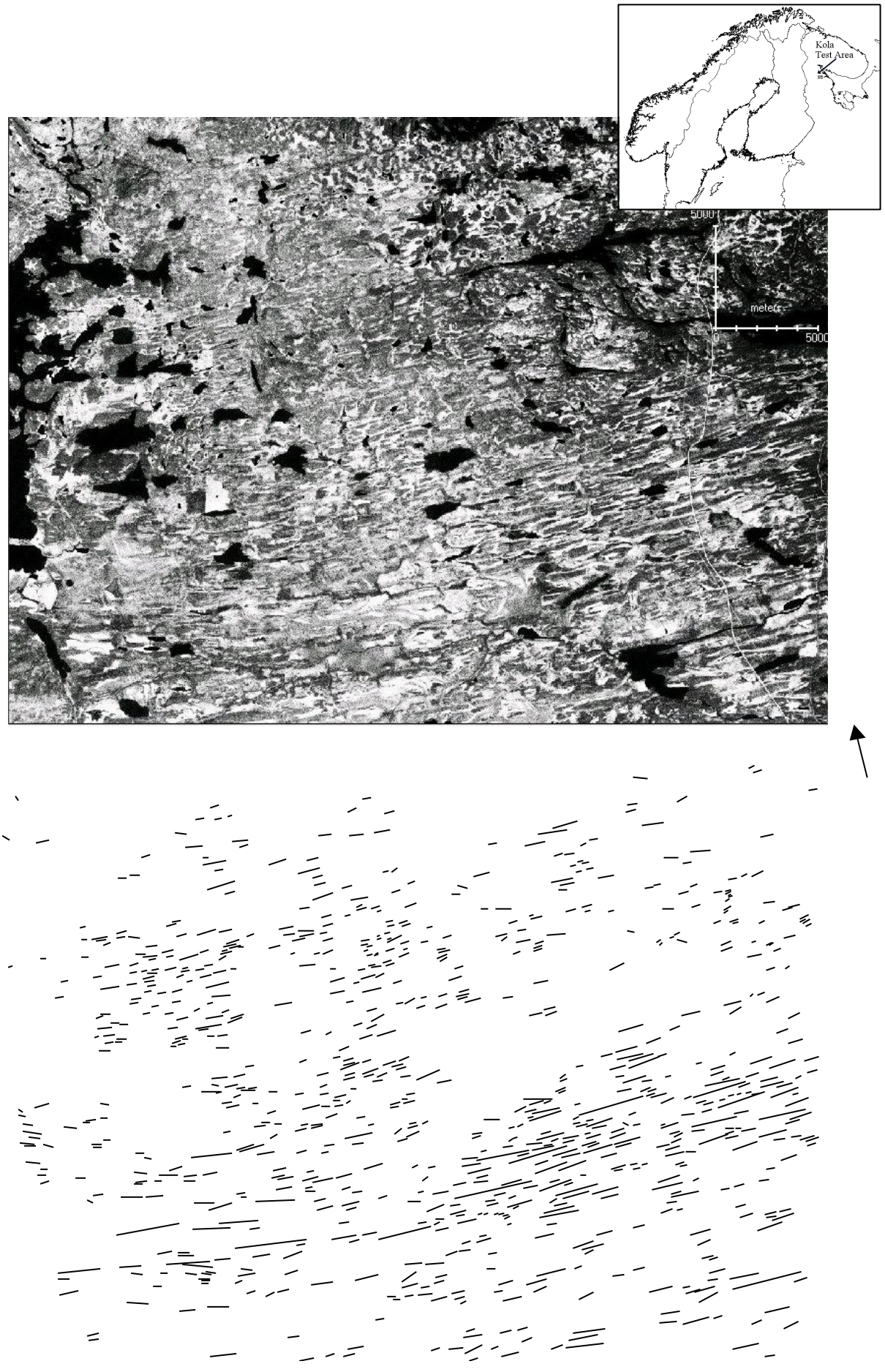

Figure 5.12a and b Landsat ETM+ Panchromatic (15m spatial resolution) image (top), and glacial lineaments mapped from it (bottom), for the Kola Peninsula, Russia. Arrow indicates azimuth angle.

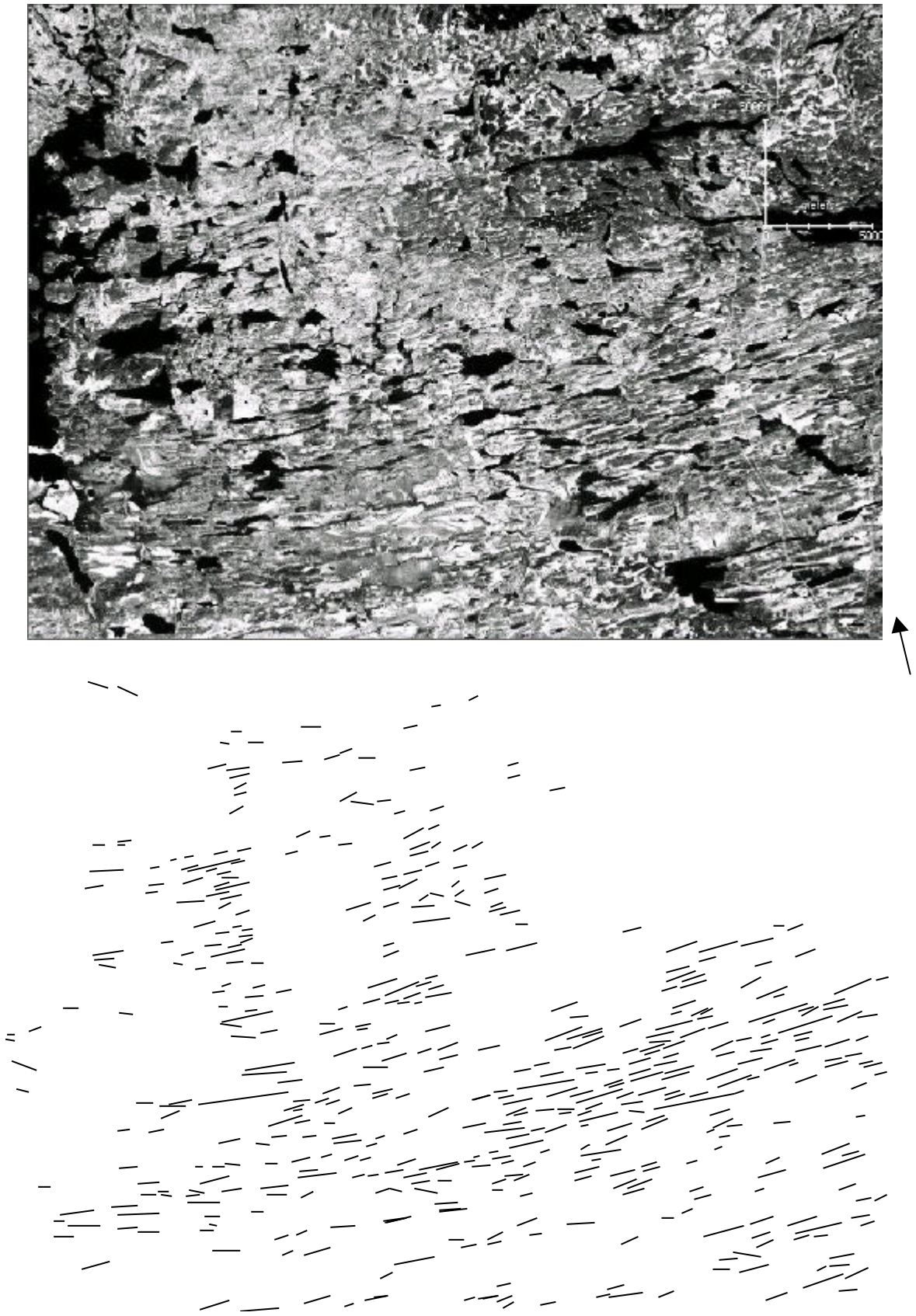

Figure 5.13a and b Landsat ETM+ Multispectral (Band 2; 30m spatial resolution) image (top), and glacial lineaments mapped from it (bottom), for the Kola Peninsula, Russia. Arrow indicates azimuth angle.

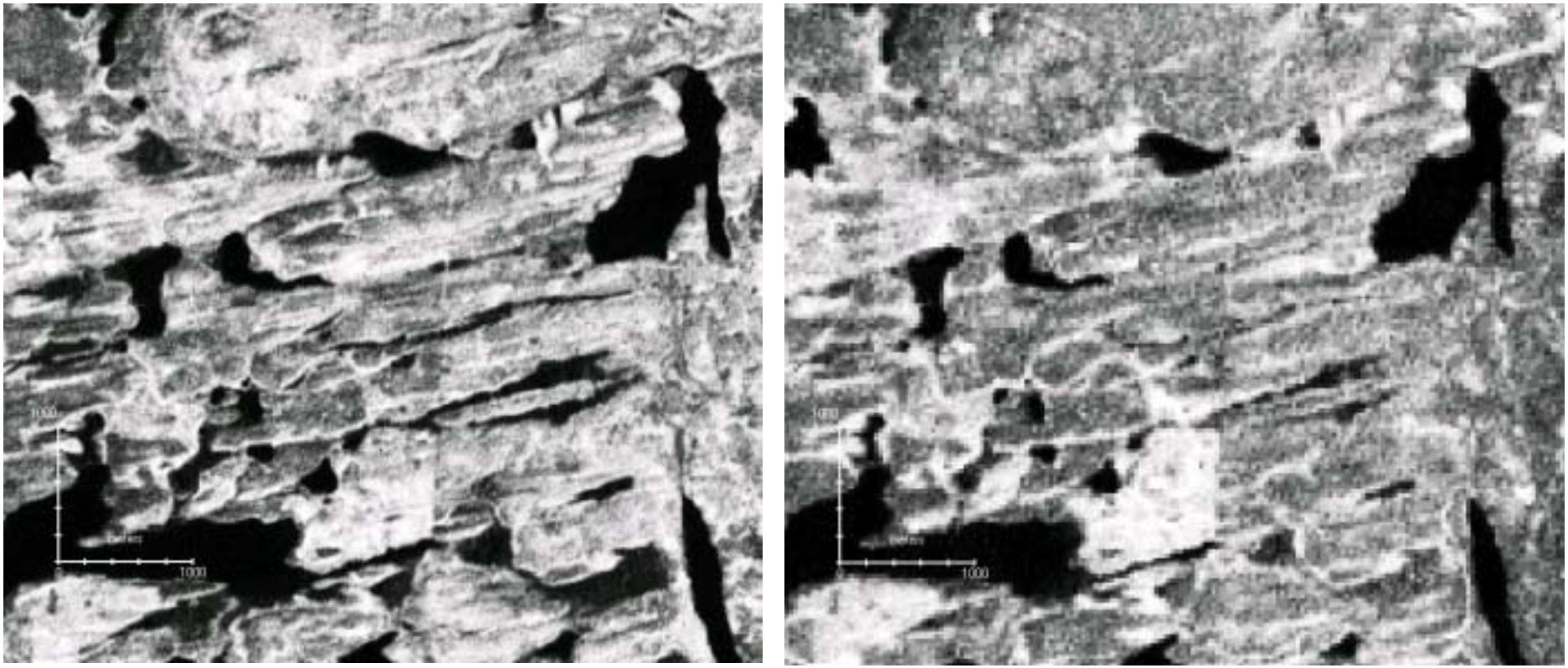

Figure 5.14a and b Zoomed sections of Landsat ETM+ Panchromatic (left) and Multispectral (right) images (Kola Peninsula, Russia) showing the effect of sensor spatial resolution (15m and 30m respectively) on lineament detection

differentiation (Figure 5.12a and zoomed image Figure 5.14a). Non-vegetated regions appear as dark areas and typically mark lineament ridges, which are often offset from elongated lakes. The high spatial resolution of the image (15m) allows clear identification of lineaments as short as 80m in length.

The mapped lineaments (Figure 5.12b) show a strong orientation of SW to NE, ranging up to 4km in length. The larger lineaments are clearly detectable, although they are sometimes composed of several, smaller, lineaments.

Multi-spectral (Band 2)

The multi-spectral image (Figure 5.13a and zoomed image Figure 5.14b) also allows lineament detection through spectral differentiation. The effect of decreased resolution (30m) is clearly apparent through the higher proportion of longer lineaments mapped. For example, where many individual lineaments might have been mapped on the panchromatic image, the multi-spectral image often shows a single, larger, lineament. The mapped lineaments (Figure 5.13b) range from 280m to 4km in length, with a strong SW to NE orientation.

5.3.2 Analysis of Controls on Detectability

In this section the lineament maps are used to infer what the main controls on lineament detectability are.

1) Landform Signal Strength

Low (11.2º) and high (48.3º) solar elevation images were acquired for the test areas (Figure 5.15a/b). These show the dramatic impact solar elevation has on lineament representation. The high solar elevation provides little tonal and textural variation, whilst the lack of surface cover variation means that the lineaments are very difficult to identify. Conversely low solar elevation selectively enhances landforms.

2) Azimuth Biasing Effect

Although it is possible for the azimuth angle to vary from due east to due west, testing its effect on landform detectability is difficult as it is not possible to hold other factors, such as solar elevation, constant. As a result it is not possible to

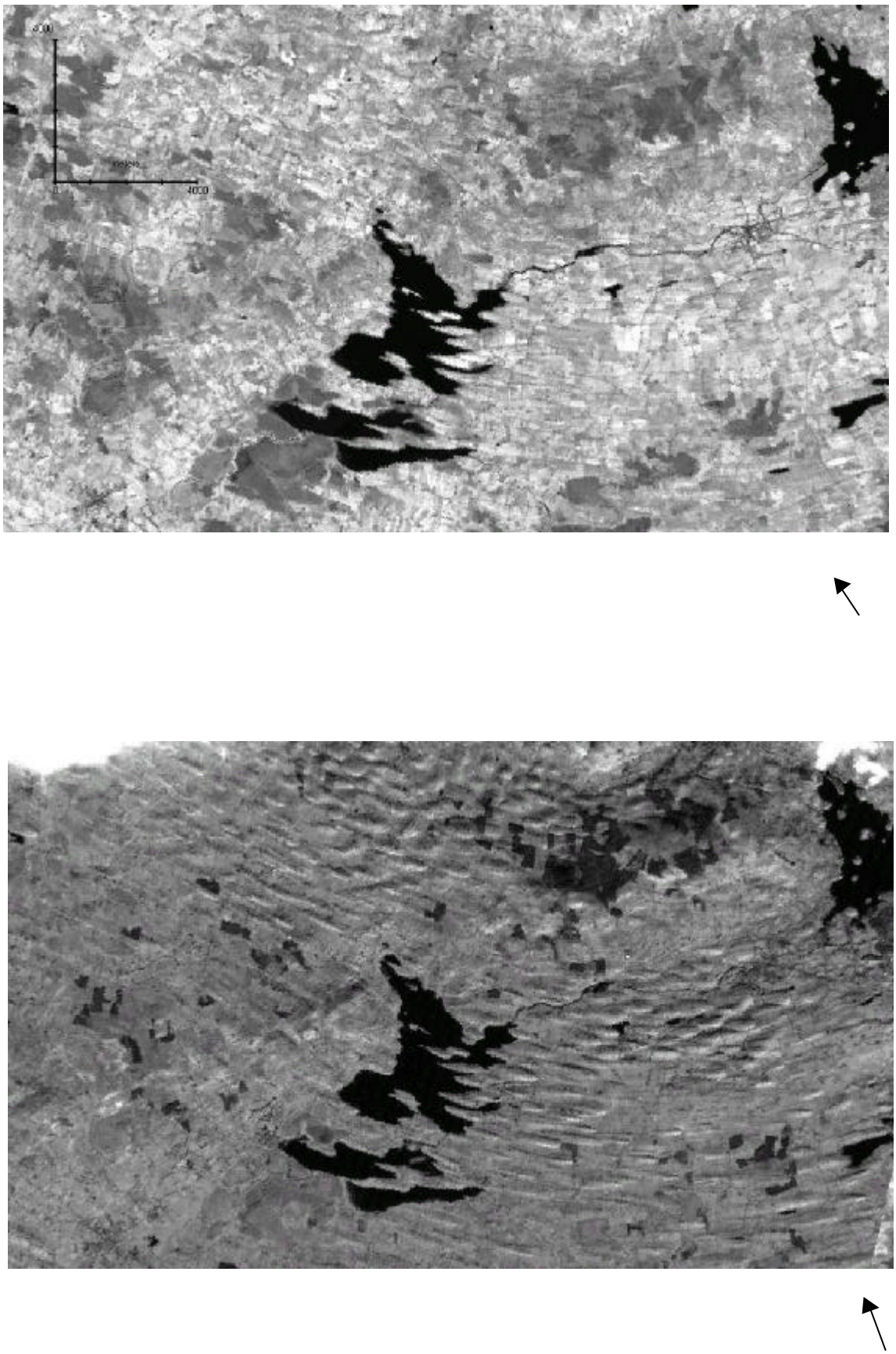

Figure 5.15a and b Landsat TM images of Lough Gara, Ireland, with a high solar elevation angle of 48.3º (top) and a low solar elevation angle of 11.2º (bottom). This illustrates the poor representation of lineaments as a result of the high solar elevation. Arrows indicate azimuth angle.

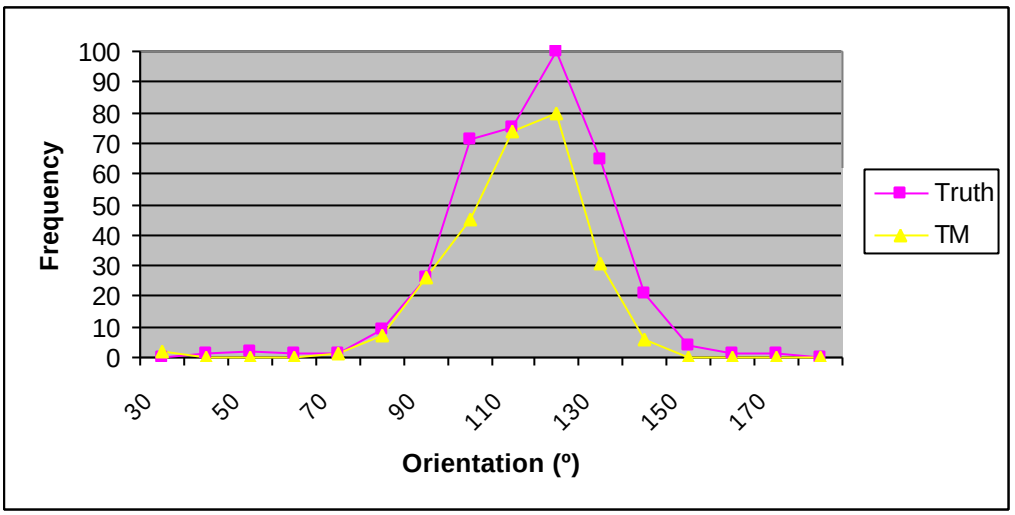

Figure 5.16 Frequency polygon of lineament orientation for Landsat TM and the truth data. Azimuth biasing is not readily apparent due to the restricted zone of lineament orientations.

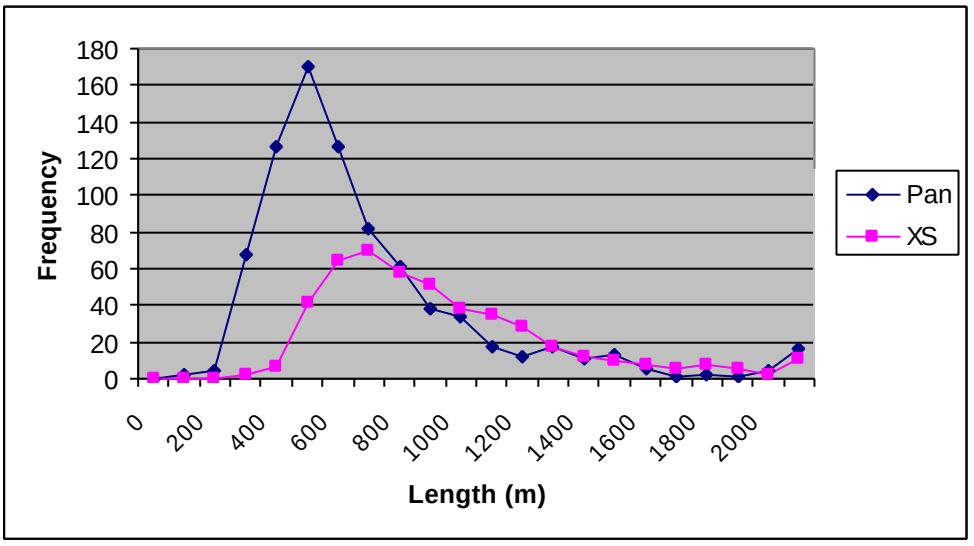

Figure 5.17 Frequency polygon of lineament length for Landsat ETM+ Panchromatic (15m; Pan) and Multispectral (30m; XS) data, Kola Peninsula, Russia. These illustrate the increased number of smaller lineaments that were mapped from the panchromatic image.

test variations in the azimuth angle using different imagery. Consequently, the effect of varying lineament orientations was used to test the azimuth biasing effect. This was achieved through the use of one image (Landsat TM) with a variety of oriented lineaments. This was then compared to truth. The Landsat TM image has an azimuth angle of 159.7º; so lineaments oriented in this direction should be selectively "hidden." Although the Landsat TM has a lower maximum lineament orientation in comparison to the truth (Table 5.2), the frequency polygon shown in Figure 5.16 shows little difference between the two data sets. This is a result of the dominant lineament direction of 110º. The mean lineament orientation for both data sets (Table 5.2) also support this.

Lineament Orientation	***Truth***	***Landsat TM***
Vector Mean *(°)*	109	107
Min *(°)*	40	24
Max *(°)*	161	135
Number	377	271

Table 5.2 Descriptive statistics of lineament orientation for truth and Landsat TM data. The higher maximum for truth data suggests the selective "hiding" of lineaments oriented parallel to the illumination azimuth.

In order to explore this effect more fully, the DEM of the Lough Gara region was relief shaded with illumination orientations parallel, orthogonal and intermediate to the principal lineament direction. Figures 5.2a and b show the DEM relief shaded using an illumination orientation parallel and orthogonal to the principal lineament direction. The difference between the two images is striking, showing not only the complete disappearance of lineaments (not visible in *parallel* that are visible in *orthogonal*), but also a change in the shape of other forms. This includes the appearance in *parallel* of transverse ridges (in the north), which have lineaments superimposed on to them.

The above description is supported by the statistics in Table 5.3. These show a dramatic reduction in the total number of lineaments mapped using a *parallel* illumination, when compared to the *orthogonal* and *intermediate* illuminations. It is also important to note that the *parallel* image identifies transverse ridges within the image and an increased number of hillocks. The transverse ridges

were identified on the aerial photography, although their morphology is subdued due to their reorientation by the overlying lineaments. As a result the *parallel* image selectively enhances these, whilst the *orthogonal* image degrades them. The increase in the number of hillocks is probably due to the misrepresentation of lineaments as hillocks and consequently their misidentification.

Landform	*Orthogonal*	*Parallel*	*Intermediate*	*Truth*
Lineament	371	176	330	442
Hillock	101	120	75	109
Transverse Ridge	0	20	0	25

Table 5.3 Total number of lineaments, hillocks and ridges mapped from the DEM for alternately relief shaded azimuth angles, illustrating the selective "hiding" of lineaments and enhancement of transverse ridges for those mapped from the *parallel* image.

3) Relative Size

Intuitively it would be expected that, as resolution increases, smaller lineaments become detectable and so more lineaments are mapped. As a result the modal lineament length (histogram peak) will gradually decrease.

Using the Landsat ETM+ Panchromatic (15m) image of the Kola Peninsula, 813 lineaments were mapped, compared to 473 lineaments for the multi-spectral (30m) image. This significant increase (170%) in lineaments can be attributed solely to the resolution of the sensor, as all other variables are constant (e.g. solar elevation, azimuth angle). Table 5.4 presents descriptive statistics for these data. This shows that in addition to more lineaments being mapped, the panchromatic image represents not only shorter lineaments, but a greater number of them. This has the overall effect of reducing the mean (from 892m to 647m) and consequently shifting the histogram peak towards the origin (Figure 5.17). In addition the total length of all lineaments on the panchromatic image have increased by 125%. This supports the above evidence, showing that there are an increased number of shorter lineaments.

Lineament Length	*Panchromatic*	*Multispectral*
Mean *(m)*	647	892
Min *(m)*	81	282
Max *(m)*	3951	4040
Total Lineament Length (km)	526	422
Number	811	472

Table 5.4 Descriptive statistics of lineament length for the Landsat ETM+ high resolution (Panchromatic: 15m) and low resolution (Multispectral: 30m) data. These highlight the greater number of smaller lineaments mapped on the panchromatic image, arising from its better spatial resolution.

5.4 Use of SAR Data

5.4.1 Introduction

This section introduces and presents details concerning the use of SAR data for landform mapping. The first section introduces some of the characteristics of radar data pertinent to mapping landforms, whilst the second section presents a case study for the area around Strangford Lough (NE Ireland), comparing and contrasting an ERS-1 SAR image with a Landsat TM image. The third section goes on to make the reader familiar with a significant amount of landform mapping that was performed over a large part of Ireland at the beginning of this research. This was begun in order to produce a glacial reconstruction of the region, however serious deficiencies were noted in the landforms visible on the imagery and the mapping was later abandoned. The final section concludes with some general comments on the use of radar imagery for landform mapping.

5.4.2 Characteristics of Radar Data

In order to understand the benefits and difficulties in using radar data, I will briefly introduce some of the main concepts involved in radar remote sensing. This research had access to an archive of satellite based ERS-1 radar data and so the discussion is based around this sensor, although the concepts can equally be applied to other radar systems. The backscatter recorded on a radar image is predominantly controlled by the following:

- wavelength
- polarization
- look angle
- signal-to-noise ratio
- dielectric coefficients

Radar (or **ra**dio **d**etection **a**nd **r**anging) is located in the microwave part of the electromagnetic spectrum. This operates over wavelengths from approximately 1mm to 1m (compared to visible light which operates between 0.4 and 0.7µm) and, because of this, has the ability to continuously record data regardless of cloud cover or night-time conditions. Although it is possible to record microwaves *emitted* by the Earth (passive sensing), emission levels are typically low and therefore active sensors (radar) are the most common. The active microwave instrumentation (AMI) aboard the ERS-1 satellite operates in the 3.75-7.5cm part of the EM spectrum (called the C band). Although this sensor can “see through” cloud cover, the wavelength can be attenuated (weakening of the signal due to absorption and scattering), particularly during heavy rain events. In these situations the rain (or shadow) may well be recorded on the image.

Polarization refers to the way the electric radar signal is filtered in relation to the direction of wave propagation. The signal can be either vertical (V) or horizontal (H) when it is either transmitted or received. This gives rise to differences in the way objects appear on imagery as they interact with V or H polarized signals differently. ERS-1 SAR imagery is VV polarization (transmitted and received with vertical polarization).

The look angle is the angle from the point directly beneath the sensor to the point of interest. As noted in §4.2, this “side looking” capability specifically highlights topography and so makes SAR particularly effective at imaging lineaments.

The signal-to-noise ratio refers to the amount of actual genuine backscatter that is recorded on an image, in comparison to areas where no return signal is received.

The intensity of radar return signals is strongly affected by the electrical characteristics of the surface being imaged. The *dielectric coefficient* is a measure of an object's reflectivity and conductivity and, for natural materials, typically varies between 3 and 8. Of importance for natural environments is that the presence of moisture significantly increases the reflectivity of a surface. Therefore the weather conditions at the time of image acquisition *and* prior to it will influence the moisture content of natural surfaces (e.g. vegetation) and so the reflectivity of objects.

Chapter 4 introduced the main controls of landform detectability. These included relative size, azimuth biasing and landform signal strength. These will now be discussed in relation to radar. Relative size is predominantly concerned with the resolution of the sensor. For ERS-1 this is nominally 25mx25m and is close to the resolution of Landsat TM data. Azimuth biasing occurs in a similar way to VIR imagery, except that illumination for the image is provided by the sensor itself so that the illumination angle is perpendicular to the flight of the spacecraft. Finally, the landform signal strength is predominantly controlled by the look angle of the sensor. This is fixed (for ERS-1), so any variability in surface reflectivity will be controlled by the surface being imaged.

In summary, the type of image recorded is controlled by the wavelength, polarization and look angle of the sensor employed. The dielectric coefficient of the surface being imaged is important and, for natural environments, will be particularly sensitive to changes in moisture content. The signal-to-noise ratio can inform us of quality of an image that is recorded.

The AMI aboard ERS-1 is designed slightly differently to other satellite based radar systems. It operates at a slightly shorter wavelength, has a relatively steep look angle and employs VV polarization. The shorter wavelength means that surface vegetation will reflect radar signals and that heavy rain events may

produce interference, whilst the steeper look angle produces less geometric distortion as a result of the side-looking sensor. Finally, the choice of polarization was taken in order to enhance oceanic reflectivity, rather than HH or HV systems which are typically employed for enhancing land based radar return signals.

5.4.3 SAR Case Study

To illustrate the complementary nature of SAR and VIR imagery, a case study using a Landsat TM and ERS-1 SAR image was performed. In order to accomplish a similar experiment to those performed for the VIR imagery it would be necessary to control 2 of the 3 variables affecting landform detectability (i.e. relative size, azimuth biasing and landform signal strength). As Landsat TM and ERS-1 SAR have very similar spatial resolutions (30m and 25m respectively), the effect of relative size (relationship between spatial resolution and lineament length) can be controlled. However it is not possible to control for the differences in landform signal strength or azimuth biasing. As a result I cannot perform the same experimentation that was used earlier in this chapter. Rather this case study is designed to highlight the benefits in using SAR imagery to detect landforms, as well as the differences with VIR imagery.

The case study was located in the Strangford Lough region of north-eastern Ireland where a descending ERS-1 SAR image and a cloud free, winter (low sun angle), Landsat TM image were acquired (meta-data are presented in Table 5.1). The images were geocorrected and then any detectable lineaments mapped.

Figures 5.18 and 5.19 depict a selected region from the SAR and TM images respectively; the dominant lineament directions for SAR (north-south) and TM (east-west) are striking, and are further illustrated by the frequency histograms of lineament orientation (Figure 5.20). Table 5.5 also supports these results showing a much higher mean lineament orientation for the ERS-1 SAR data.

These results are principally explained by the difference in azimuth angle between SAR and VIR imagery. SAR imagery is obtained by active detection

using a sensor angled obliquely, orthogonal to the satellite track. As the satellite is polar-orbiting, this means that all images are sensed in an easterly or westerly direction depending on whether the satellite is in an ascending or descending orbit. Consequently all lineaments oriented approximately north-south are selectively enhanced, whilst those oriented approximately east-west are selectively degraded (Graham *et al*, 1991).

Lineament Orientation	*SAR*	***Landsat TM***
Vector Mean *(°)*	145	105
Min *(°)*	0	3
Max *(°)*	179	167
Number	289	349

Table 5.5 Descriptive statistics of lineament orientation for ERS-1 SAR and Landsat TM data for the Strangford Lough region, highlighting the different populations of lineaments (with different orientations) mapped.

5.4.4 Landform Mapping of Ireland

The research for this thesis was initially concerned with producing a glacial reconstruction of the United Kingdom and Ireland. Project feasibility was to be tested through a pilot study involving a large proportion of Ireland for which ERS-1 SAR satellite imagery had previously been acquired specifically for this purpose. Ireland contains one of the largest drumlin swarms in Europe and, as a result, is an important area for lineament research. Given the good preservation of glacial bedforms in the landscape, there should be plenty of evidence on which to base a geomorphological glacial reconstruction. In addition, the fact that the Irish ice sheet is thought to have been almost entirely separate from the British mainland (although there is evidence of marginal influence from the Scottish Uplands) means that it can be studied as a small, self-contained, unit.

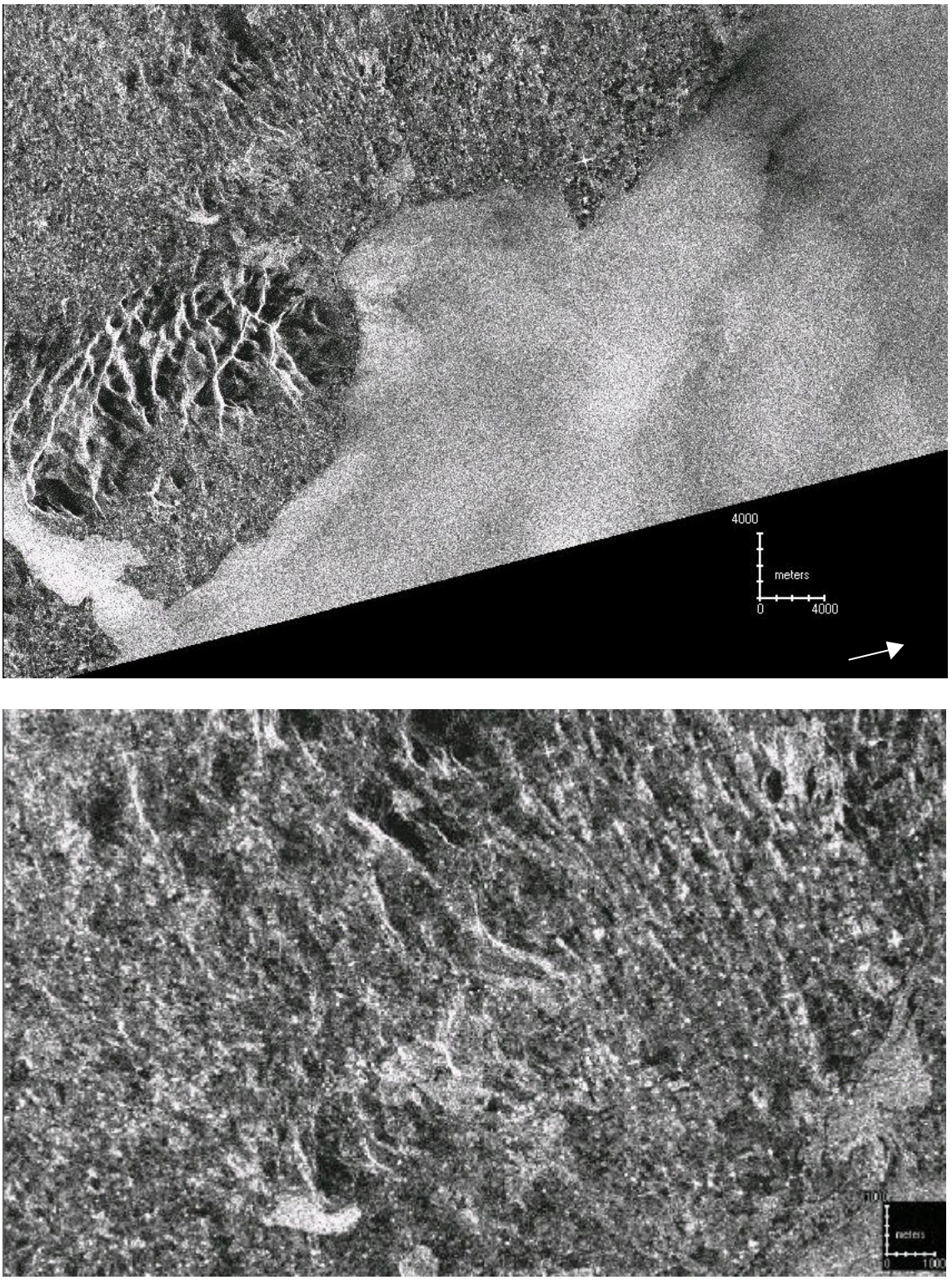

Figure 5.18a and b ERS-1 SAR image (top) of Strangford Lough, Ireland. In conjunction with Figure 5.19, note the dramatic effect of the azimuth angle on lineament representation. Image b is a zoomed region. Note that the E-W trending lineaments on the Landsat TM (Figure 5.19) image are not visible on the ERS-1 SAR image. Arrow indicates the azimuth angle.

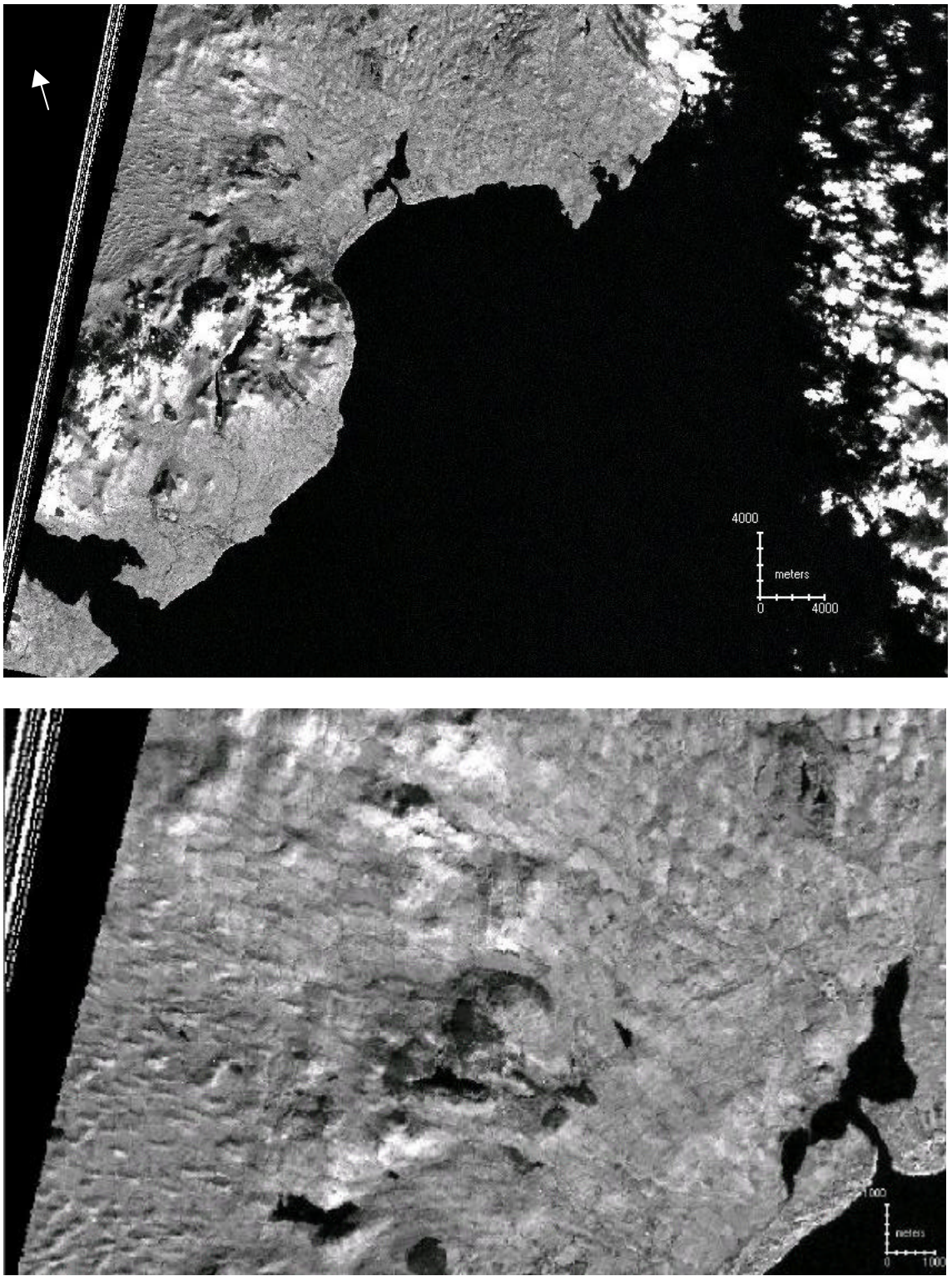

Figure 5.19a and b Landsat TM image of Strangford Lough, Ireland. In conjunction with Figure 5.18, note the dramatic effect of the azimuth angle on lineament representation. Image b is a zoomed region. Note that the E-W trending lineaments on the Landsat TM (Figure 5.18) image are not visible on the ERS-1 SAR image. Arrow indicates the azimuth angle.

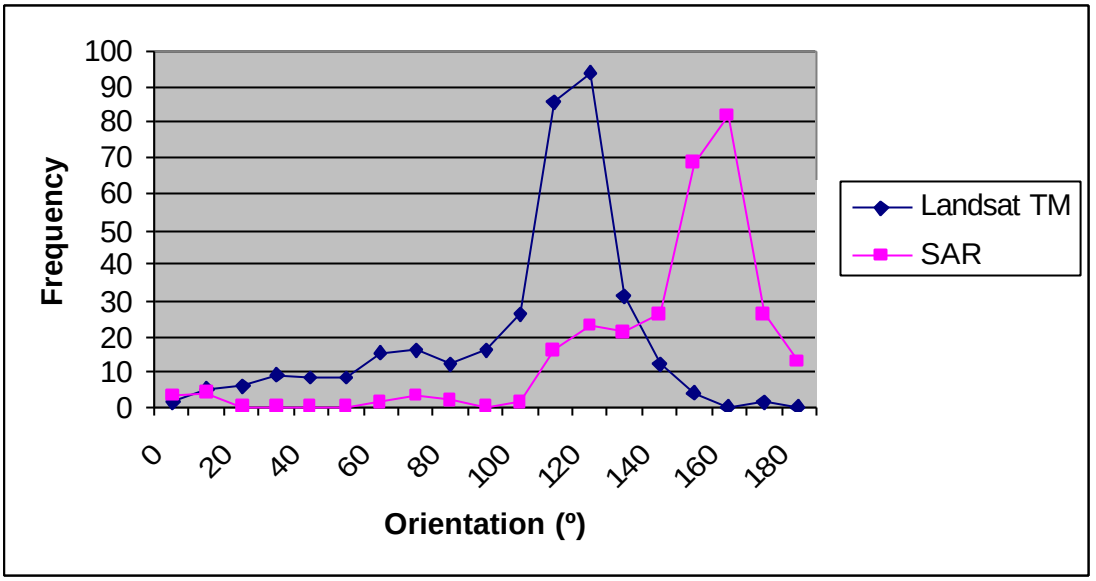

Figure 5.20 Frequency polygon of lineament orientation for Landsat TM and ERS-1 SAR data, illustrating the completely different populations of lineaments (with different orientations) mapped for Strangford Lough, Ireland.

Having acquired the relevant SAR imagery and applied the pre-processing techniques outlined by Clark (1997), mapping was performed using the same methods employed earlier in this chapter. Figure 5.21 depicts all the lineaments mapped for this part of the project. These patterns have been outlined, in parts, by various authors but never mapped in their entirety. Figure 5.22 provides an example of the type of summary mapping that has been performed. This is a generalised view of the authors review of data from various field and aerial photography mapped sources, as well as personal experience. Much of the published evidence for lineaments fails to recognise the presence of cross-cutting in the landscape and therefore this summary highlights dominant lineament patterns around the country. Many of these patterns will have occurred at different times and trying to synthesise this information is virtually impossible.

In Chapter 1 I outlined the impetus for the research in this thesis and this included the generally poor landform representation of ERS-1 SAR imagery in Ireland. The remainder of this section reviews the lineament mapping performed in Ireland and summarises the reasons for its poor performance.

In reviewing Figure 5.21, the first point to note is that ERS-1 SAR coverage of Ireland is **not** complete. Imagery was not obtained for southern Ireland, although few drumlins are known to exist in this region (Warren, 1992). However in the remainder of the country a variety of small areas were missed due to lack of coverage. For example, the rectangular band running across the middle of the country lies *between* two images. Likewise, small areas in the west, north-west, north-east and east also remain uncovered. The area in the east turns out to be quite critical as a significant number of bedforms can be found in this area (Clark and Meehan, 2001).

Figure 5.21 depicts several areas that are noticeable due to the parallel conformity of the mapped landforms. An example of this is Donegal Bay (outlined on Figure 5.21); Figure 5.23 shows a zoomed section (a) of this area, with the lineaments mapped from it (b). The lineaments are clearly defined on

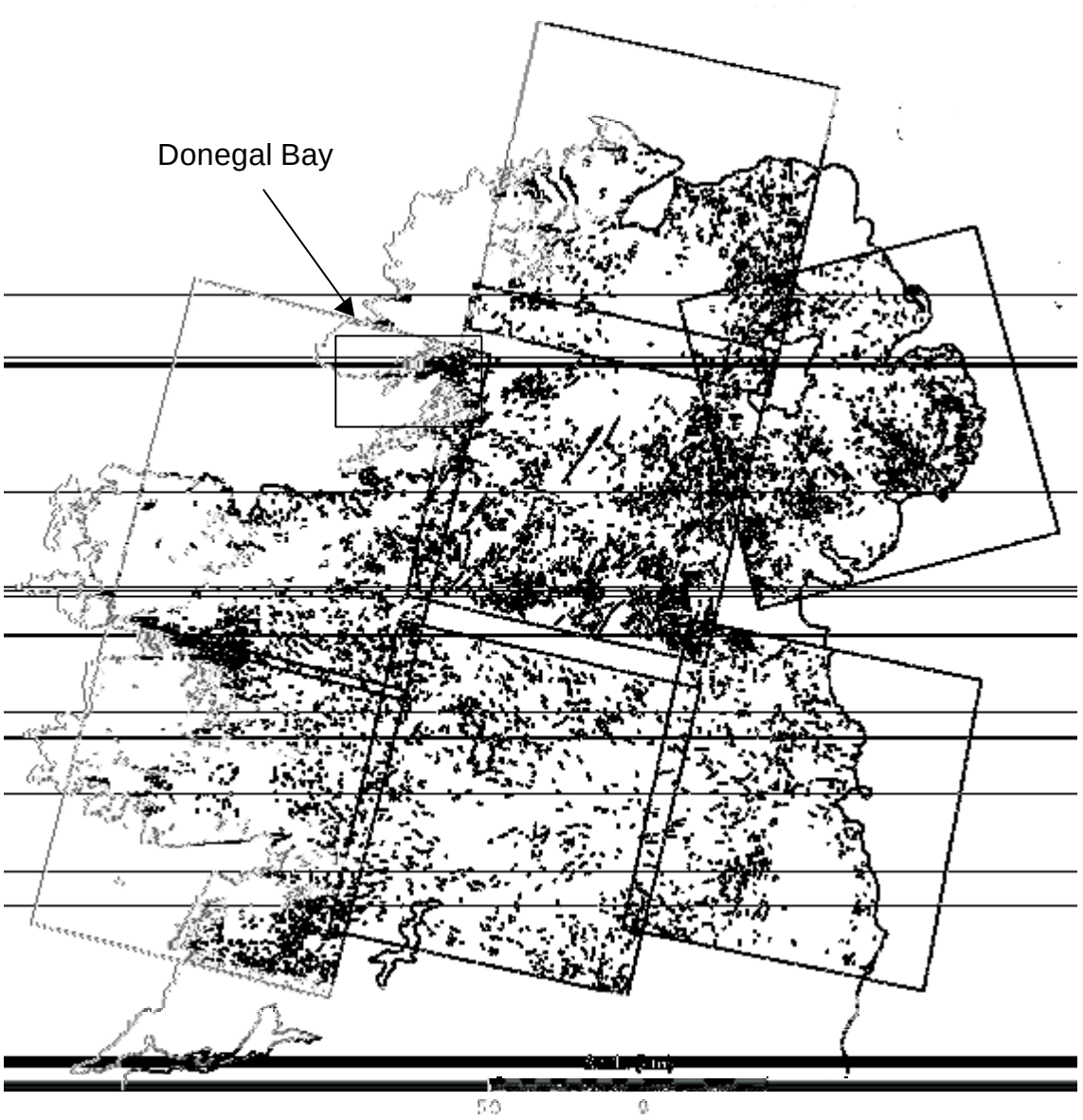

Figure 5.21 Lineament mapping from ERS-1 SAR satellite imagery (including an outline of the SAR image coverage and locations noted in the text). Whilst good quality mapping can be verified (e.g. around Clew Bay), there are many areas where lineament mapping is poor.

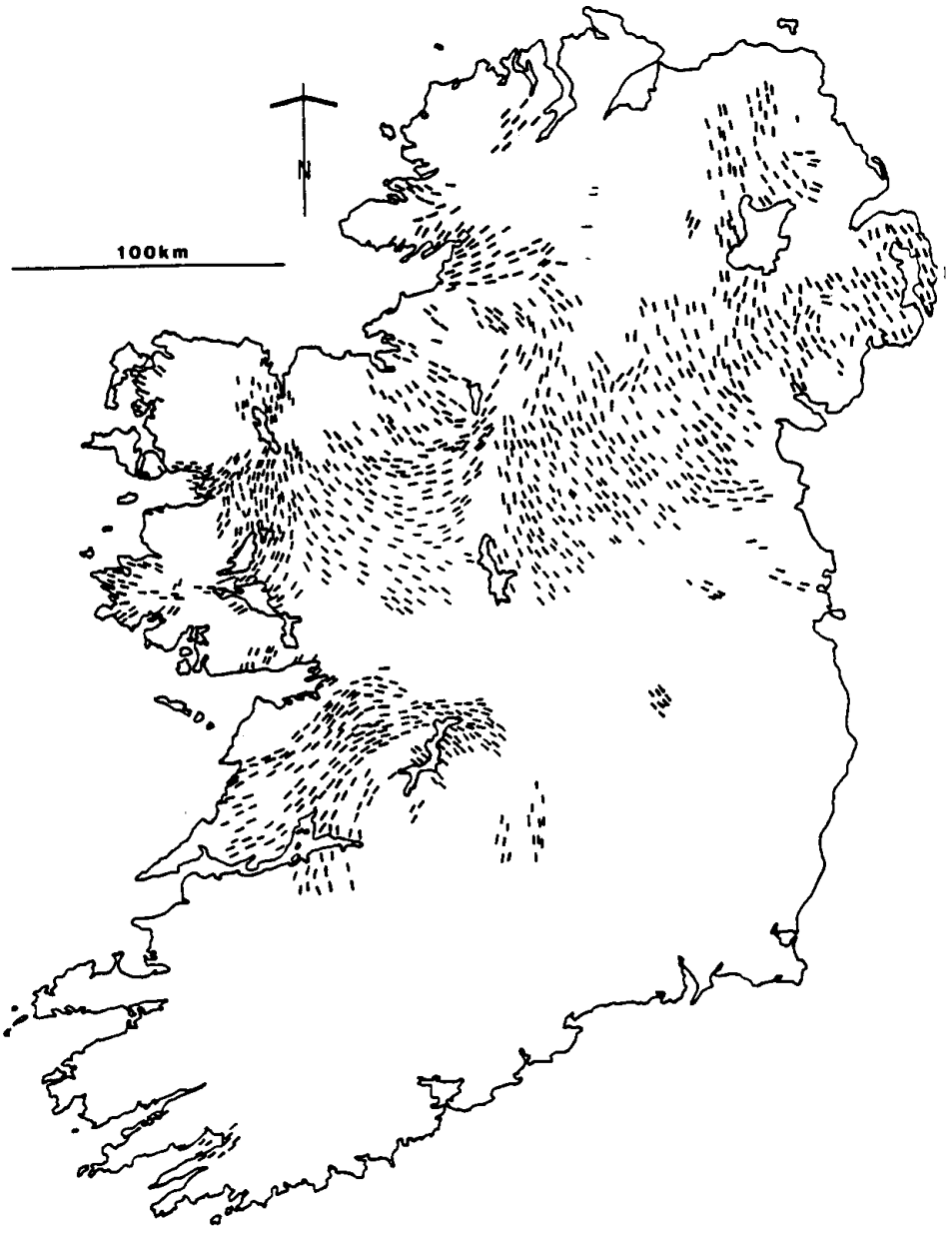

Figure 5.22 Generalised distribution and alignment of drumlins in Ireland, as after Warren (1992).

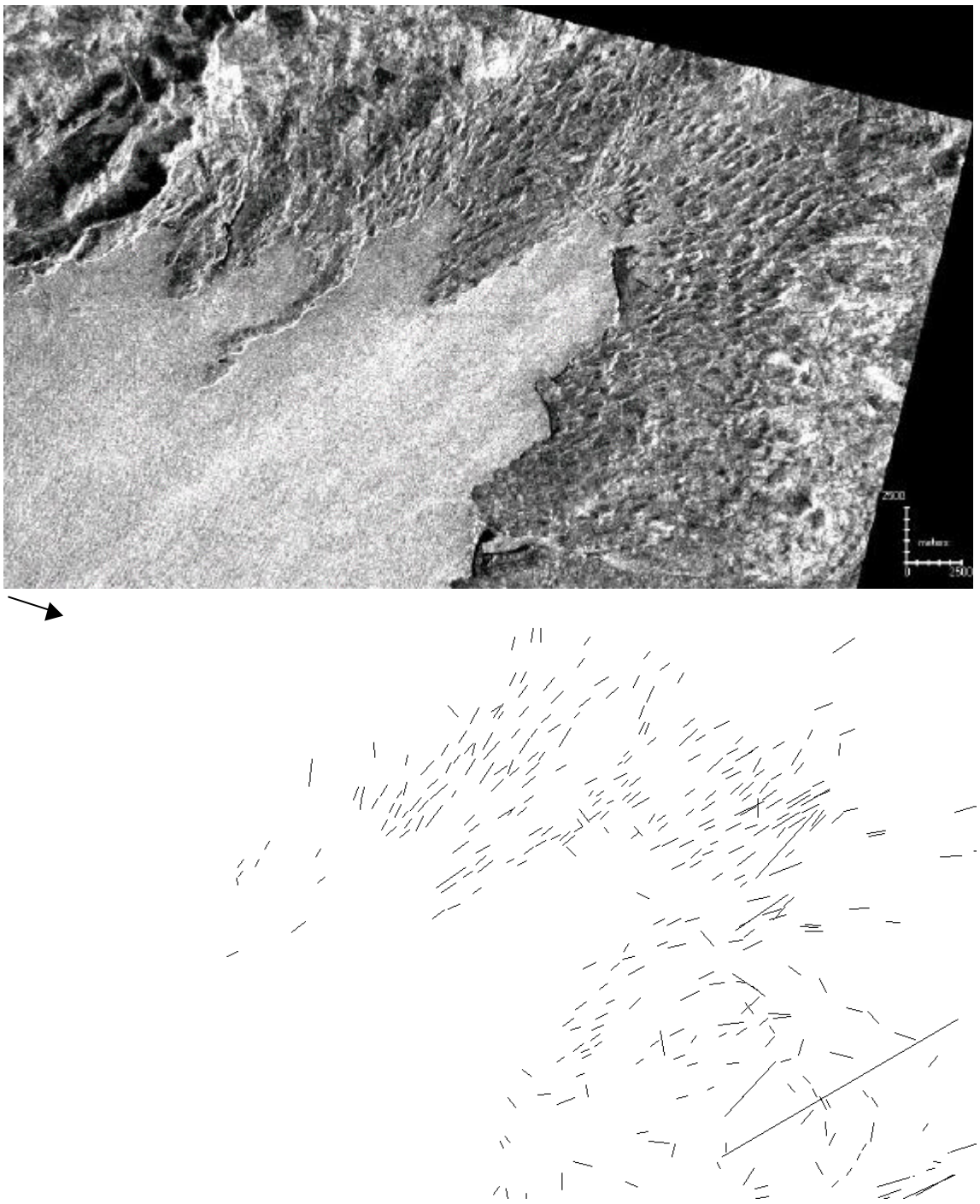

Figure 5.23 a and b ERS-1 SAR image (top), and glacial lineaments mapped from it (bottom), for Donegal Bay, Ireland. Arrow indicates azimuth angle.

the image and easy to map. This is in contrast to other areas that show no preferred orientation (e.g. central regions). Figure 5.24 shows an area around Lough Sheelin, County Cavan. This again demonstrates the *complementary* nature of SAR imagery. In the north of the ERS-1 SAR image, lineaments are strongly defined, whilst in the south they are poorly defined. The opposite is true of the Landsat TM image.

In comparison to Figure 5.22 the differences are very distinctive. The areas of high parallel conformity are similarly matched in Figure 5.21, however much of the remaining areas are very different. The SAR mapping shows lineaments that are well represented, whilst failing to identify lineaments which have been mapped on Figure 5.22. In addition, particularly in the midlands, there appear to be a large number of “spurious” lineaments.

There is undoubtedly reasonable lineament representation on parts of the SAR imagery acquired for Ireland, yet many questions remain about the overall quality of the product. This has to be placed within the context of successful use of SAR by other researchers. Knight (1996) successfully applied ERS-1 SAR mapping to the glacial landforms of the Ungava Sector of the former Laurentide Ice Sheet, whilst Ford (1981) showed high quality imagery from SEASAT-1. Although not detailed, Punkari (1985) described the utility in using Soviet airborne radar.

5.4.5 Conclusions

It is appropriate to explore some of the reasons why ERS-1 SAR data has proved so unreliable in Ireland. It is also worth commenting on the same factors that effect the VIR imagery: relative size, azimuth biasing and landform signal strength. The resolution of ERS-1 SAR data is relatively good and so moderate size lineaments should be easily distinguishable, however cross-cutting relationships will almost certainly **not** be visible. Azimuth biasing, as discussed in the previous section, strongly influences the representation of landforms on an image and is probably the main cause of differences between ERS-1 SAR and Landsat TM images. Landform signal strength, for SAR sensors, is linked to the look angle of the sensor. This is fixed for ERS-1 SAR, being relatively steep.

Although this reduces geometric distortion, it is less likely to highlight subtle topographic features.

Other factors that will effect the SAR image include the sensor wavelength, sensor polarization and surface characteristics. The wavelength of ERS-1 SAR will interact with both surface vegetation and severe rain events. If a region is heavily forested then the signal return will record the reflectance of the vegetation canopy **not** the terrain surface. Likewise, the VV polarization is designed to enhance oceanic, rather than land surface, reflectivity (Lillesand and Kiefer, 2000). The final area that is likely to affect the SAR image are the surface characteristics. These are principally the dielectric coefficient and geometric arrangement of the surface. An increase in the moisture content will increase the reflectivity of an object, particularly vegetation. The roughness of the surface will also affect reflectivity. In general, smooth, or *specular*, surfaces reflect incident radiation directly *away* from the sensor and so there is minimal backscatter. Conversely rough objects (and this will include urbanised areas) will have a much higher degree of backscatter.

These general comments provide some insight into the specific case for Ireland, however, as noted above, researchers have demonstrated that radar imagery is a good tool for mapping glacial landforms. Ford worked in limited parts of Ireland, whilst Knight acquired imagery for parts of the former Laurentide ice sheet. Clearly azimuth biasing is a major problem for SAR, but this is also the case for the other VIR imagery reviewed in this chapter. The most likely explanation is the combination of surface cover, moisture content and sensor design of ERS-1. Humankind has had a long residence time in Ireland and, over that period, the landscape has been cultivated and urbanised. In rural areas, the vegetation cover will dominate the way backscatter is returned subordinating topographic variation. Ireland also has relatively large amounts of precipitation and so high moisture content, and hence reflectivity. The wavelength used by ERS-1 SAR is designed to interact with this type of surface cover. Likewise, in urban areas there will be high backscatter. Both of these areas will tend to over-ride the subtle underlying topographic signal that is recorded as a result of the look angle of the sensor (i.e. subtle lineaments are less likely to be visible).

In comparison to Knight's (1996) study area (sub-Arctic Canada), most of the landscape has no urbanisation or agriculture and so there is still a strong association between surface cover and landforms. In addition, inter-drumlin areas in this cratonic region are likely to act as collection areas for moisture, further helping the delineation of the lineaments.

Overall SAR imagery was found to be inappropriate for mapping glacial landforms for large parts of Ireland. It is unfortunate that a large amount of mapping was required in order to highlight this effect. However, globally, other regions may have greater success. The side-looking geometry of the sensor is still able to detect subtle topographic variations and it is possible that an alternative satellite sensor may well produce imagery better suited to detecting lineaments. For example, JERS-1 operates in the L-band (23cm) and would therefore be more likely to record the actual topographic surface rather than vegetation.

With practice, good results can be obtained using SAR imagery for glacial landform mapping (e.g. Knight, 1996). This was not the case for our test area (see also §5.6) around Lough Gara where azimuth biasing and a degraded topographic signal reduced the representations of landforms on the image. However an awareness of these issues has allowed the successful use of radar imagery, utilising the benefits of consistent, "any weather", data acquisition.

For poleward latitudes, the ascending and descending paths of near polar orbiting satellites cross at high angles. This is illustrated in Ireland with ascending paths having a sensor azimuth ~104º, whilst descending paths have ~256º. By obtaining both sets of imagery for an area, azimuth biasing can be reduced, however two sets of mapping would be required.

5.5 Case Study: Lough Gara Satellite Imagery

The lineaments mapped from the Landsat MSS, Landsat TM, SPOT and SAR imagery for Lough Gara are now used to supplement the inter-image comparisons with quantitative data and so highlight the errors and bias often

present within imagery acquired for landform mapping. These are illustrated through discussion of landform signal strength, azimuth biasing and relative size, including a review of the flow patterns generated from the mapped data. The SAR image is necessarily discussed separately within each section as a result of the different inherent characteristics of the sensor. In addition, discussion of coincidence between lineaments mapped from each image type is also provided.

5.5.1 Landform Representation

The landforms mapped from the different satellite imagery are subject to the three main controls on landform representation. The effect of each of these variables is discussed in turn in order to highlight, for this series of images, the main control on representation.

Landform signal strength has an important impact on lineament representation (§4.2), however the solar elevation angles for the VIR images of Lough Gara are all similar (Table 5.1) and so can be assumed to make little difference to landform representation.

The effect of *azimuth biasing* can be significant, as illustrated by the SAR case study (§5.5). For the Lough Gara area, the lineaments are predominantly oriented in an east-west direction (as illustrated in truth). As the VIR imagery are predominantly illuminated from the south they are effectively able to display the landforms. As the images were acquired at a similar time of year, the illumination azimuths are similar and so there is little variation in landform representation as a result of azimuth biasing.

The SAR imagery is very different to the VIR imagery, with a very small number of lineaments mapped as illustrated by Figure 5.6a (and described in the inter-image comparisons). Inspection of lineament orientations shows that they have a comparable mode and range to those mapped from truth (Figure 5.25). Intuitively I would expect azimuth biasing to occur as the illumination orientation of 104º is close to the histogram peak of 120º. This appears not to be the case,

although with a relatively small sample size it is possible that such an effect is hidden.

The main difference in landform detectability between the VIR images relates to *relative size* (i.e. spatial resolution), given the minimal effects of landform signal strength and azimuth biasing. Table 5.6 shows an increase in the number of mapped lineaments as spatial resolution increases; this is demonstrated by the low number of landforms mapped from Landsat MSS (128) and the higher numbers mapped from Landsat TM (275) and SPOT (284), when compared to truth (398). Figure 5.26 presents a frequency polygon of the total number of lineaments mapped from each image. This demonstrates that as sensor resolution increases, so the number of lineaments mapped increases and their size decreases. This may disguise the fact that, although higher resolution imagery resolves more, shorter, lineaments, lower resolution imagery may still be able to resolve (although less well) these same lineaments as fewer, contiguous, lines. Table 5.2 also presents total lineament length for each image, a measure designed to remove the effect of fragmentation of mapped lineaments. This highlights the poor ability of SAR and Landsat MSS to satisfactorily resolve lineaments, whilst Landsat TM and SPOT are clearly better. Interestingly Landsat TM has the longest total lineament length of all the imagery suggesting that it is able to resolve all the lineaments visible on SPOT, although more fragmentation occurs on the latter. As a result Landsat TM appears to be satisfactory for lineament mapping, but higher resolution imagery may be necessary in order to resolve cross-cutting relationships.

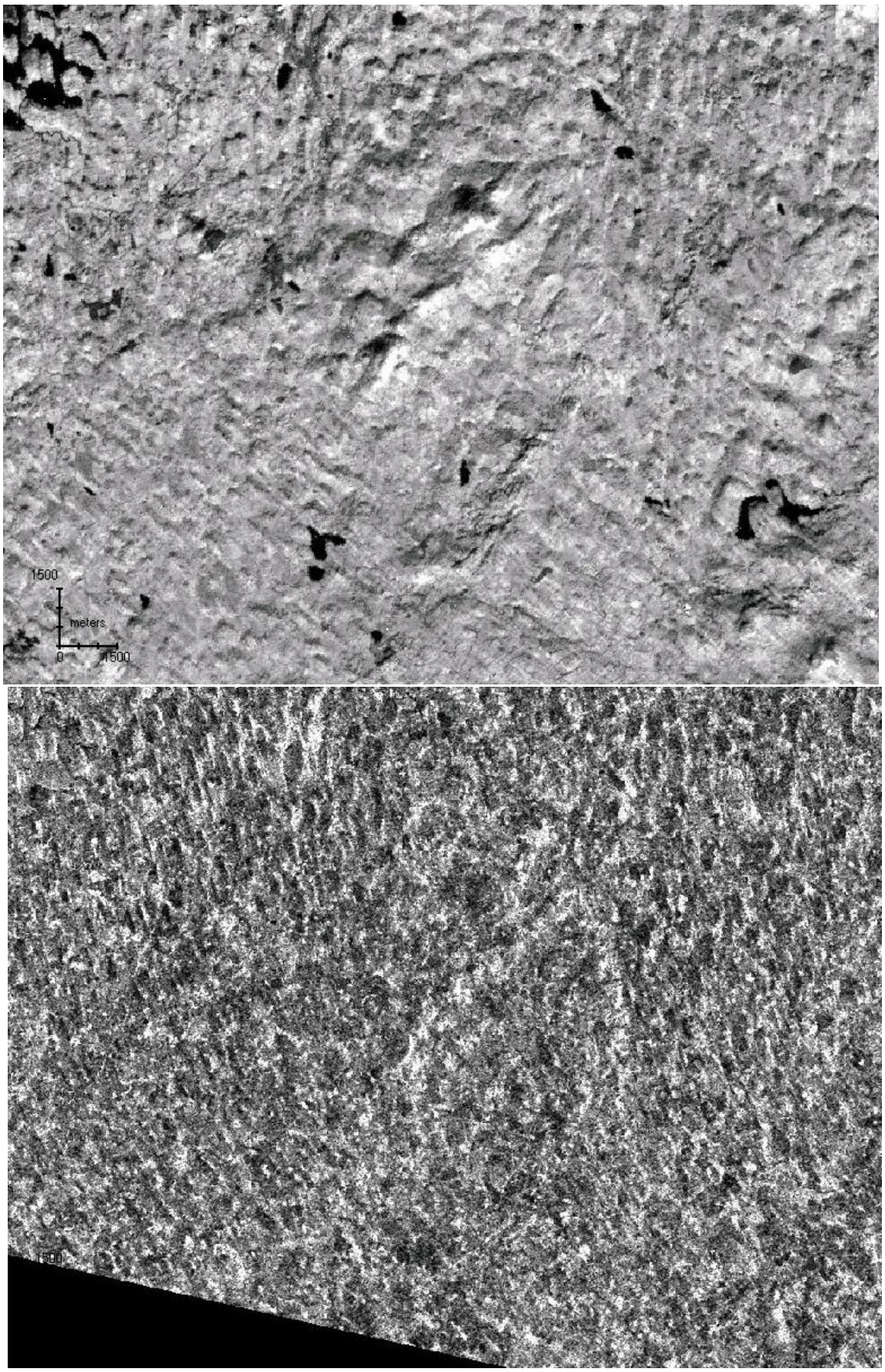

Figure 5.24 a and b Landsat TM image (top) and ERS-1 SAR (bottom) around Lough Sheelin, County Cavan, Ireland. Note the strong representation of lineaments in the north of the SAR image *absent* on the TM image and vice versa.

Region	Image (resolution)	Total Number of Lineaments	Total Number of Hillocks	Total Lineament Length (km)
Ireland	Landsat MSS (80m)	128	30	93
	Landsat TM (30m)	275	47	194
	SPOT (10m)	284	27	166
	ERS-1 SAR (25m)	75	49	58
	Truth (50m)	398	101	230
Russia	Landsat ETM+ Pan (15m)	813	-	526
	Landsat ETM+ XS (30m)	473	-	422

Table 5.6 Total number of lineaments and total lineament length mapped from each of the image types.

Finally, in terms of an ice sheet reconstruction, flow patterns, generalised from individual lineaments (Chapter 2), are the most important elements as they are the *non-interpreted* building blocks used to interpret the morphological data and guide ice sheet reconstruction. Any differences between datasets is unimportant as long as the flow patterns are consistent and correct. Figures 5.2, 5.3, 5.5, 5.7 and 5.9 include overlays of flow patterns for the respective imagery. All overlays are shown comparatively in Figure 5.27. Not surprisingly, the greater the number of mapped lineaments, the easier it is to generalise them into flow patterns. In addition there is more detail in the orientation of flow patterns, as well as the presence of cross-cutting. Therefore the SPOT imagery is able to highlight the curving flow in the southern portion of the image, as well as the detailed cross-cutting in the northern section. Although this level of detail is missing from the Landsat MSS imagery, similar flow patterns are still able to be drawn. The flow patterns from the SPOT and Landsat TM imagery are very similar to those from truth, however the SPOT image additionally has the presence of transverse ridges which were not identified on the Landsat TM. The poorest results were obtained from the SAR imagery. Flow patterns for the northern area are similar to those from the VIR imagery, however the southern area is poorly represented.

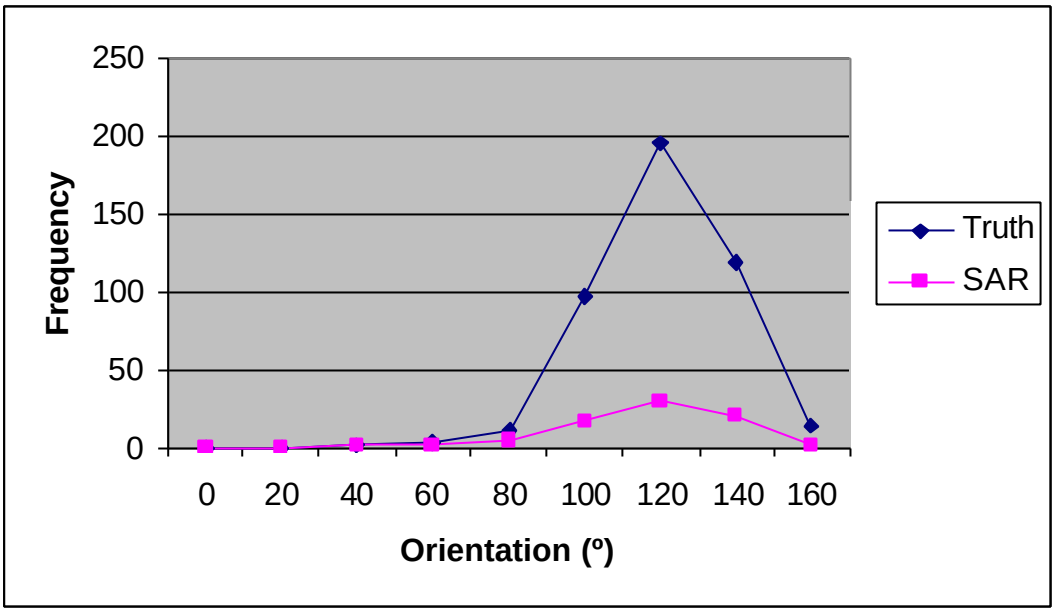

Figure 5.25 Frequency polygon of lineament orientation for ERS-1 SAR and the truth data. Although far fewer lineaments have been mapped from the SAR image, lineaments have a similar mode and range of orientation.

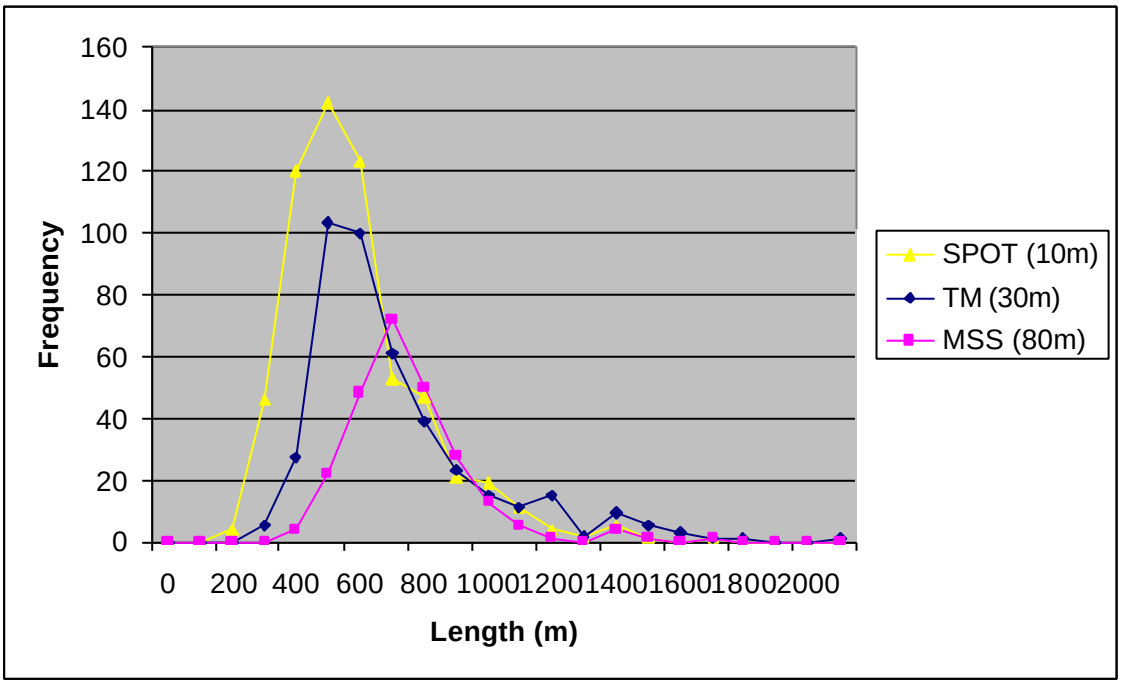

Figure 5.26 Illustration of the effect of sensor spatial resolution on the total number and distribution of lineaments mapped from satellite imagery. The frequency polygon shows that as resolution increases, so the number of lineaments mapped increases, the size of lineaments decrease and the population peak shifts towards the origin.

5.5.2 Lineament Coincidence

In addition to reviewing the different spatial bias effects on VIR imagery, it is also appropriate to consider the degree of coincidence in lineament mapping between the different imagery and the truth. Coincidence was assessed visually with lineaments required to be within approximately 200m of each other and not deviate by more than 15º. Visual assessment was selected as the optimum method as consideration could be given to any deviations a result of poor digitising or varying geocorrection. Mapped lineament overlays are visually presented in Figures 5.28-5.33.

Each VIR image is overlaid on to truth (Figures 5.28-30), with relevant statistics provided in Table 5.7. These show the number of lineaments coincident with lineaments on truth, hillocks coincident with lineaments, the total coincident lineament length and the percentage of lineaments (on truth) coincident with each image. In general there is an increase in the number of coincident lineaments (column 1) as the spatial resolution of the sensor increases. The number of coincident hillocks (column 2) remains fairly constant, showing similar azimuth biasing between image types, irrespective of resolution. Total coincident lineament length (column 3) also increases with sensor resolution. Finally the percentage coincidence (taking into account hillock/lineament coincidence; column 4) increases with spatial resolution. As a final note the SAR imagery can be seen to perform very badly with only 9% coincidence and a small 19km total coincident lineament length.

Image	Number of Coincident Lineaments	Number of Coincident Hillocks	Total Lineament Length (km)	Lineament Coincidence (%)
Landsat MSS	69	23	47	22
Landsat TM	178	11	134	47
SPOT	197	14	117	51
ERS-1 SAR	23	13	19	9

Table 5.7 Number of coincident lineaments, number of coincident hillocks and total lineament length, with the truth, for each image type. The final column shows the percentage of lineaments on *truth* that are coincident with each image type.

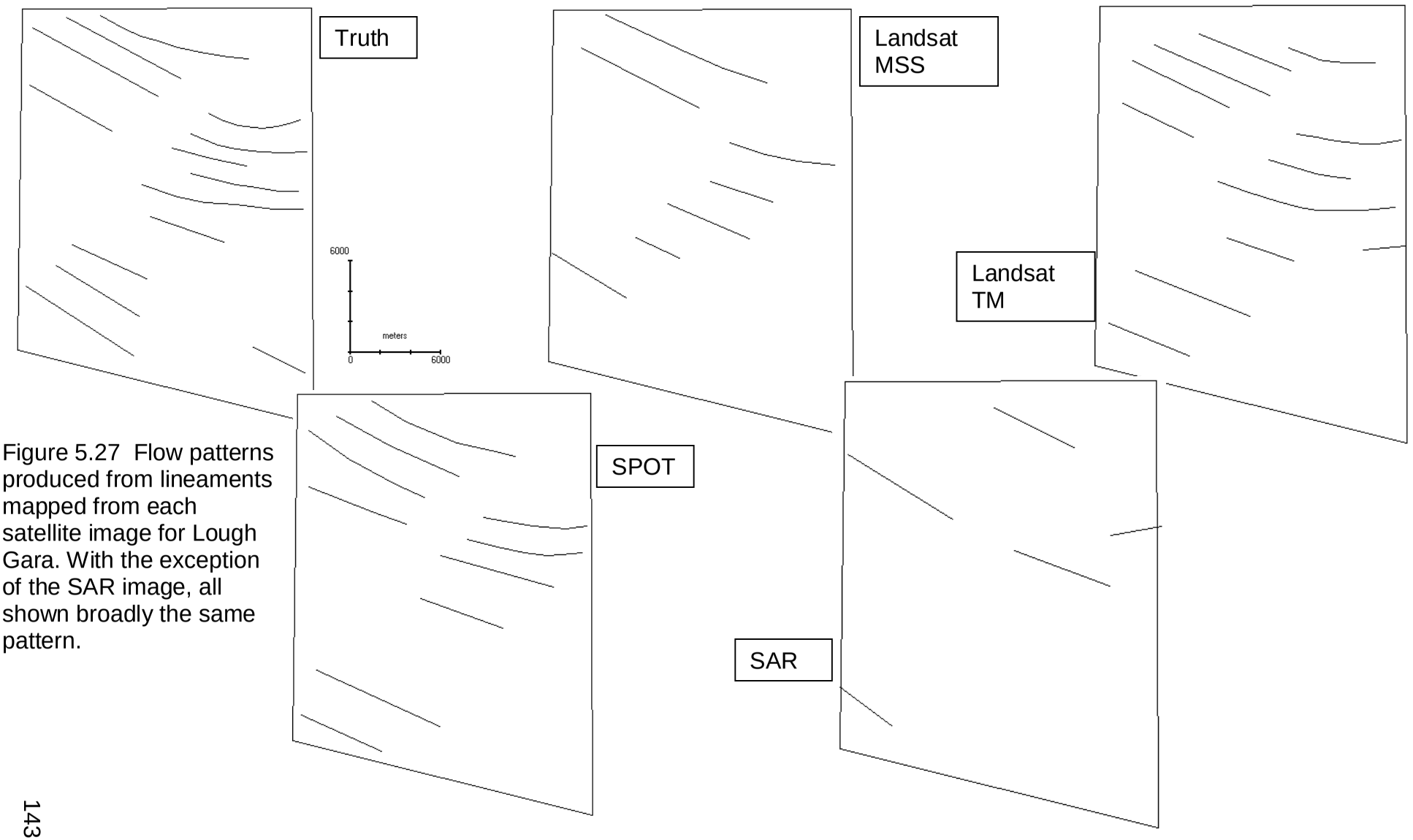

Figure 5.27 Flow patterns produced from lineaments mapped from each satellite image for Lough Gara. With the exception of the SAR image, all shown broadly the same pattern.

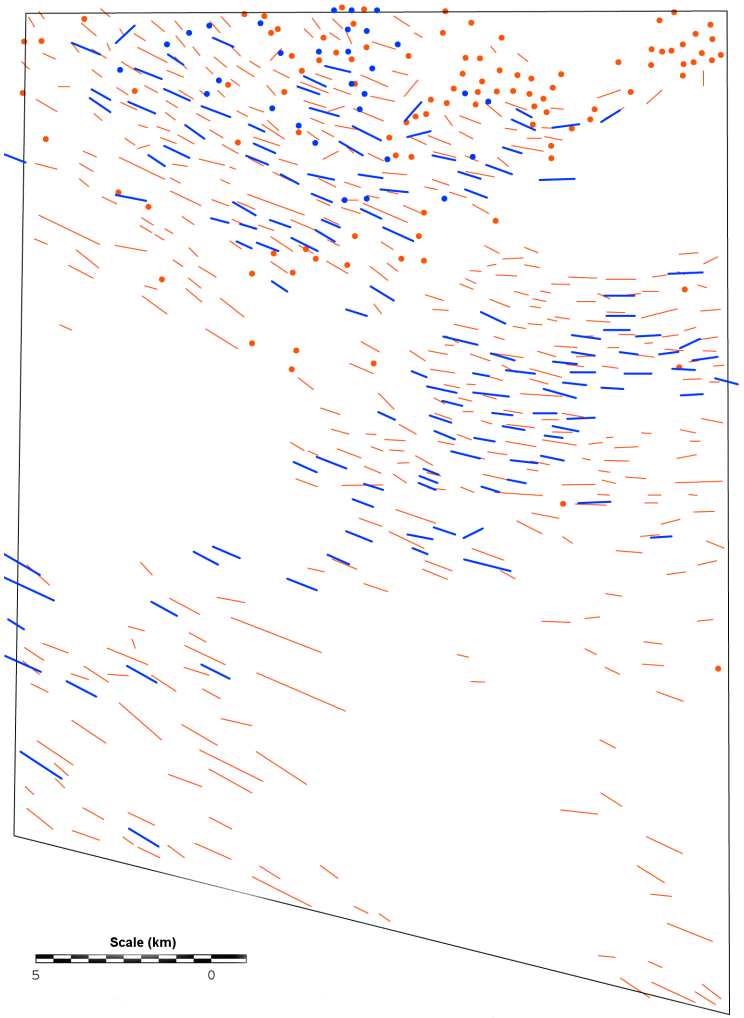

Figure 5.28 Overlay of lineaments and hillocks mapped from Truth (red) and Landsat MSS (blue) imagery.

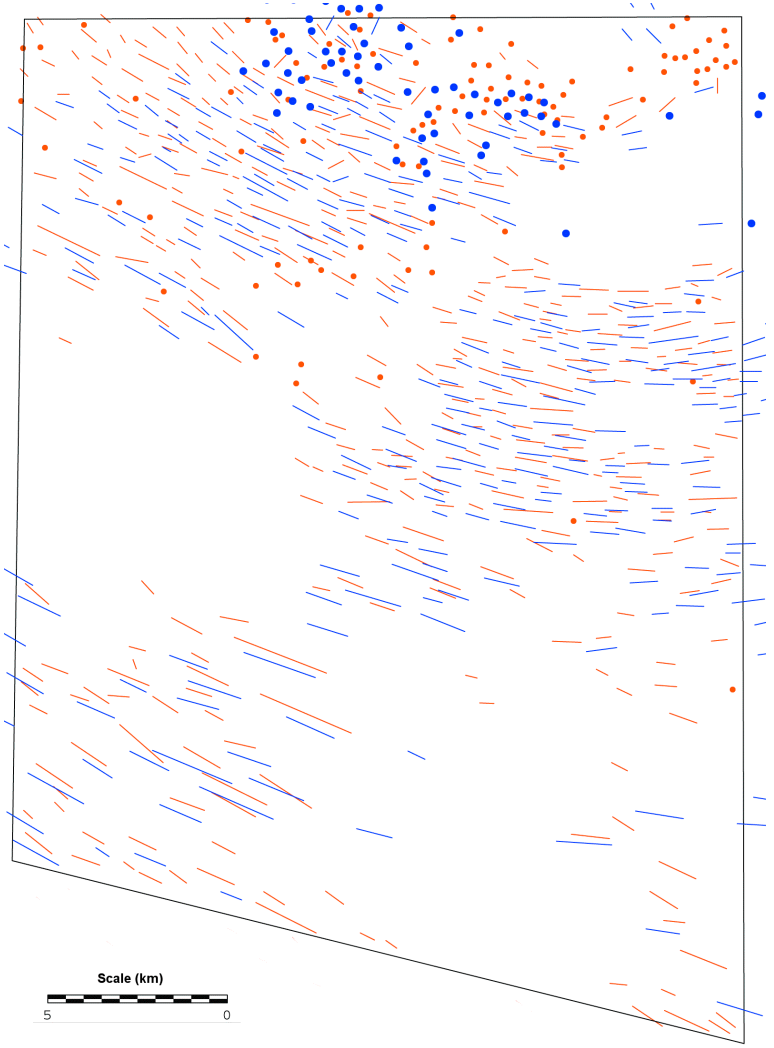

Figure 5.29 Overlay of lineaments and hillocks mapped from Truth (red) and Landsat TM (blue) imagery.

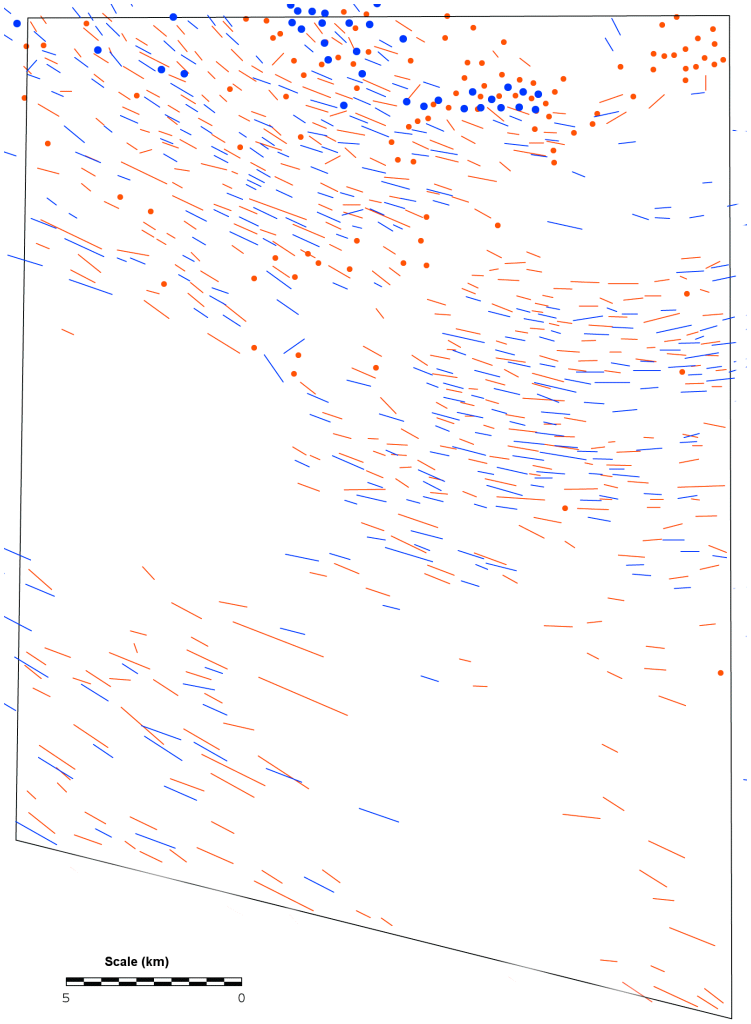

Figure 5.30 Overlay of lineaments and hillocks mapped from Truth (red) and SPOT (blue) imagery.

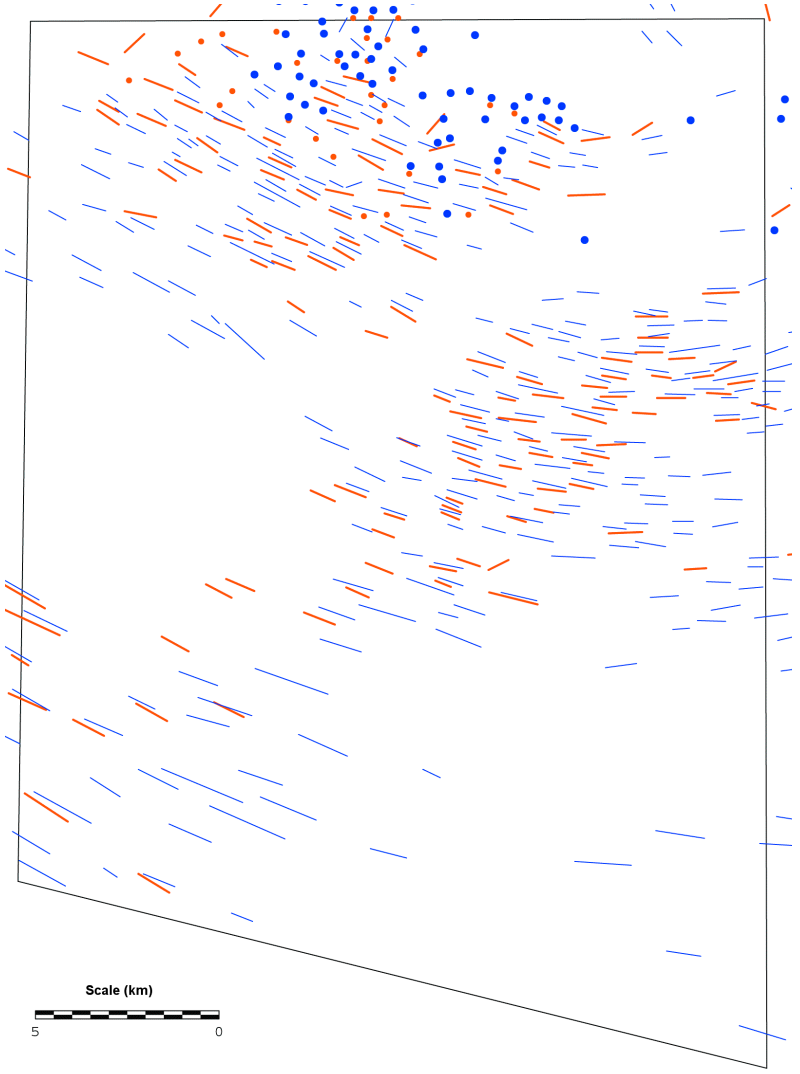

Figure 5.31 Overlay of lineaments and hillocks mapped from Landsat MSS (red) and Landsat TM (blue) imagery.

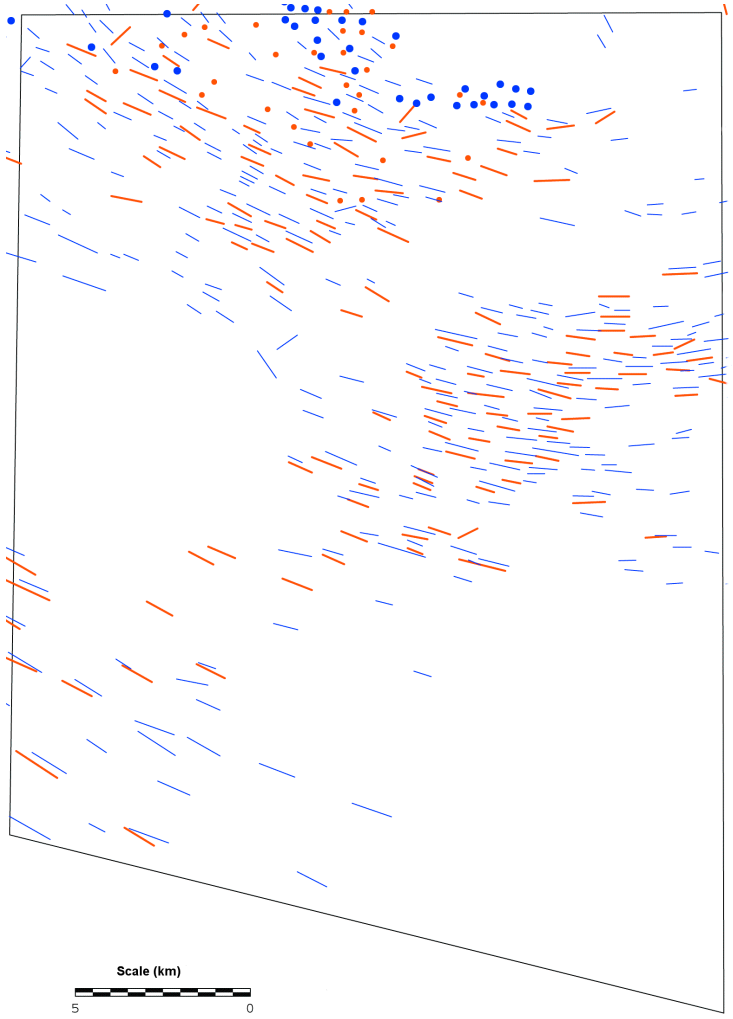

Figure 5.32 Overlay of lineaments and hillocks mapped from Landsat MSS (red) and SPOT (blue) imagery.

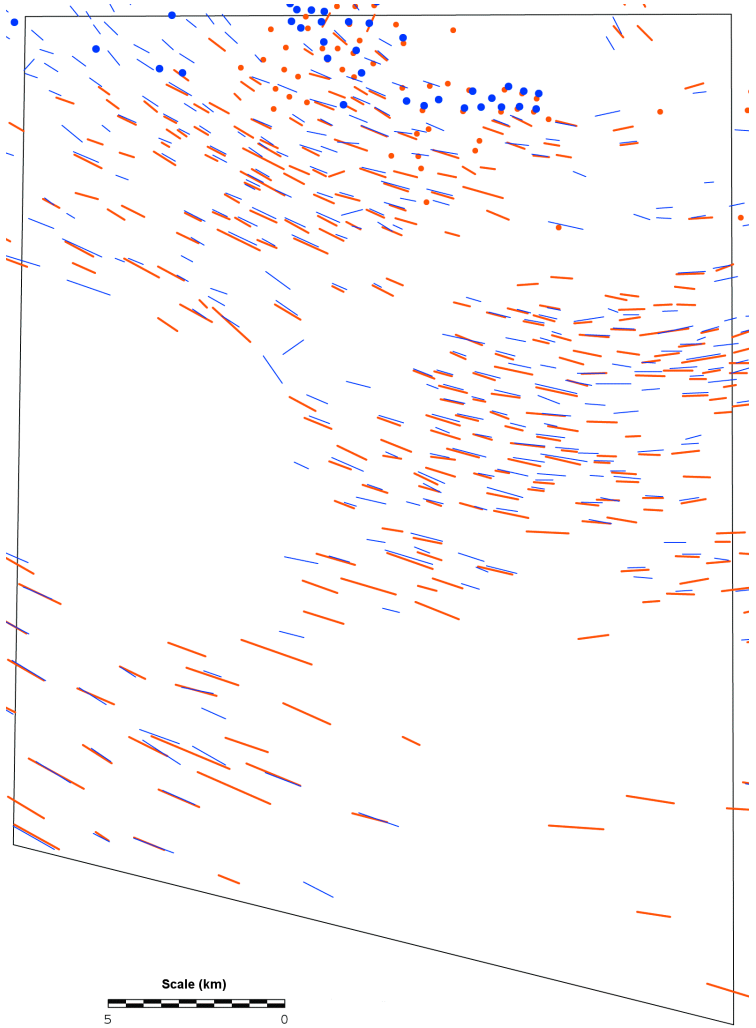

Figure 5.33 Overlay of lineaments and hillocks mapped Landsat TM (red) and from SPOT (blue) imagery.

Individual inter-image comparisons were performed and summarised for the VIR imagery in Figures 5.31-5.33, with summary statistics in Table 5.8. The results are not surprising in that over 70% of lineaments on Landsat MSS are coincident with those on SPOT and Landsat TM. SPOT and Landsat TM are also highly coincident, a product of their high spatial resolution. Again however, there are 20-30% of lineaments that are generally not coincident (e.g. 30% of lineaments on Landsat MSS are not coincident with those on Landsat TM), comprised of varying orientation, length and location. This can only be accounted for by geocorrection, mapping and comparison errors.

	Landsat MSS	Landsat TM	SPOT
Landsat MSS		50	40
LandsatTM	70		73
SPOT	78	82	

Table 5.8 Percentage spatial coincidence of lineaments between the VIR satellite images. For example, 70% of lineaments on Landsat MSS are coincident with those on Landsat TM

In summary, for this particular area, azimuth biasing and landform signal strength do not contribute major elements of bias for VIR imagery. Relative size has the single largest affect on mapped lineaments, whilst geocorrection, mapping and comparison errors probably account for the remaining variability. The SAR imagery is strongly affected by azimuth bias and is a poor data source for lineament mapping in this instance.

5.6 SummaryandRecommendations

This chapter has described the benefits in using satellite imagery for glacial landform mapping. However these benefits have to weighed against weaknesses in its use. There are two main areas where error can be incorporated into a landform map (where there is a primary focus on lineament mapping). These are inherent bias within the imagery acquired and the ability of the observer to map the landforms. The latter has been touched upon by several authors whilst the former is the topic of this chapter.

Image bias can occur from relative size, azimuth biasing and landform signal strength. The effect of each of these variables on lineament mapping has been

investigated for study areas in the Lough Gara region of western Ireland and the Kola Peninsula, Russia.

The results suggest that low solar elevation is required (for VIR imagery) in order to selectively highlight landforms (e.g. see Figures 5.5b and 5.6). From experience it is advised to obtain imagery with a solar elevation below ~20º, although <15º is desirable. Depending on latitude, solar elevations as low as 5º are possible. For Landsat ETM+, daylight imaging is not performed for solar elevations below 5º. Above 20º there is a gradual decrease in the relief effect and tonal variation to a point where lineaments are only detectable by surface cover variation. The availability of appropriate imagery from archive is variable, depending upon the latitude of the study area and the sensor desired. In mid-latitudes, winter scenes are necessary in order to acquire a low solar elevation and, coupled with the requirements for scenes to be snow and cloud free, makes suitable imagery difficult to obtain. In high latitudes, summer imagery is required in order acquire snow free scenes, although this is not necessarily ideal as solar elevation can be quite high (Table 5.1). Aber *et al* (1993) suggest that light snow cover, in association with a high relief effect, can increase detectability as tonal variation due to surface cover is effectively masked. This has to be weighed against the possible reduction in the relief effect with increased snow depth. Subtle landforms can quickly become “hidden” making mapping of features such as cross-cutting landforms difficult.

Perhaps the single greatest bias, over which the observer has little control, is the azimuth biasing effect. Both the SAR case study and the DEM experiments suggest that large omissions and misidentification can occur as a result of azimuth biasing. More particularly, the above constraints on acquisition dates for VIR imagery produce a small solar azimuth window through which images are available. As a consequence, lineaments oriented parallel to the azimuth are selectively diminished, such that they may change shape, appear as hillocks or completely disappear. It is important to be familiar with a study area in order to be aware of this problem; for some areas no action may be necessary as lineaments may not be oriented in this direction. However other areas may require the acquisition of alternative data sources in order to mitigate

against this error. These sources include local mapping in the form of topographic maps, digital elevation models or field mapping. Where these are not available SAR imagery can be usefully used. Its alternative viewing geometry satisfactorily supplements VIR imagery, although mappers should not underestimate the experience required in its use (see Vencatasawmy *et al,* 1998 for further discussion).

The final bias, relative size, is familiar to most researchers. The higher the resolution of the satellite imagery, the greater the ability to map smaller landforms. The above results show a 170% increase in mapped lineaments by moving from 30m resolution data to 15m data. However higher precision data does not necessarily mean better quality results and it is important that researchers select imagery to match the requirements of their project. For ice sheet reconstruction, overall lineament trend is the single most important element. As a result, azimuth effects are the most serious problem since they can introduce a selective bias into the mapping. In contrast, relative size and solar elevation are less important than azimuth bias here, since the errors produced should be distributed randomly across lineaments of all orientations. From a more practical perspective, it is useful if the image coverage is as large (and cheap!) as possible. High resolution data are desirable if detailed or cross-cutting mapping are intended. Equally, multi-spectral data are very useful as they can be used to delimit lineaments through surface cover changes. These requirements point to Landsat ETM+ as the optimal images, given the near-global coverage, large scene area (180x180km), high resolution (15m panchromatic) and multi-spectral facilities. In addition, the open access policy of NASA make the data very cheap. The disadvantage, in the short-term, is the short mission run-time which means, for mid-latitude regions, that suitable imagery may not yet be available.

If Landsat ETM+ data are not available for a particular region, then the choice of imagery becomes more difficult. SPOT are available in both high resolution panchromatic and multi-spectral formats, but the scene coverage is small (60x60km) and relatively expensive. Landsat TM has had a longer mission time and so suitable imagery may be available that takes advantage of the larger

areal coverage and multi-spectral format. Although cheaper than SPOT, Landsat TM is considerably more expensive than Landsat ETM+ and has a lower resolution (in equivalent panchromatic mode). Finally, Landsat MSS has had a very long mission time (and consequently large archive) and benefits from the areal coverage and multi-spectral format of the other Landsat missions. However it suffers from relatively poor spatial resolution.

As a result, it is recommended that Landsat ETM+ is used wherever suitable imagery is available. Otherwise, SPOT is desirable for geomorphological or cross-cutting mapping over small areas. If mapping glacial landforms over larger areas then Landsat TM is the best alternative, particularly where more detailed information on cross-cutting is required. Finally, Landsat MSS has great utility in the large archives and low cost that make it appropriate for small-scale mapping within tight budget constraints, or as a reconnaissance tool.

The acquisition of appropriate imagery requires identifying the desired sensor and selecting cloud free imagery that has low solar elevation and little snow cover, as well as being aware of the solar azimuth and any biasing that might occur.

The most suitable dates for image acquisition are dependent upon latitude, satellite overpass time and the satellite repeat cycle. Ideally it would be good to pinpoint an approximate date when viewing conditions are optimum and then search for cloud free imagery. The accompanying CDROM contains two Microsoft Excel ™ spreadsheets which allow the user to do just that. They contain complete overpass time and latitude/longitude data for Landsat ETM+.

The first spreadsheet presents solar azimuth and elevation angles (accurate to 0.5°) for every Landsat ETM+ grid cell (termed World Reference System or WRS) on the first day of every month. Appendix 2 explains the calculation of solar elevation and azimuth in more detail, with a worked example.

The overpass times use a sample set of data from the year 2000, however they can vary by ±5mins due to the degradation of orbit the satellite suffers through

the year. This degradation is corrected on an annual basis. The overall affect on the calculation accuracy is minimal for the purposes of identifying the most suitable acquisition dates. Given this data, the user can locate which month is the most appropriate to obtain data.

The second spreadsheet contains the overpass time and latitude/longitude data, along with the necessary equations to calculate solar azimuth and elevation, allowing the user to make their own calculations if necessary.

Figure 5.33 presents a graphical illustration of the variation in solar elevation and azimuth for the Landsat ETM+ scene of Lough Gara, Ireland (WRS 207.23). January and December are clearly the best months to obtain imagery with low solar elevation, however days in these months are often cloud covered. The solar elevation then rises to a peak of ~60º in June and July. Solar azimuth also varies from ~145º to ~165º.

In addition to the use of satellite imagery, this chapter has shown that DEM data can be effectively used to map landforms. Researchers should be aware of the impending arrival of a variety of different, satellite based, DEMs. SRTM data is now partially available at 90m and 30m spatial resolutions. The 90m data will be publicly available, whilst limited non-USA 30m data will be available to researchers upon application. Data from a second sensor (owned by the German and Italian space agencies) was also used to produce a further DEM and this will be available for commercial purchase. Researchers will find, however, that there will still be large regions that lie outside the SRTM coverage area. In addition, the use of C-band radar by SRTM means that the true ground elevation may not be calculated in vegetated areas due to interference. With the launch and operational status of NASA's Terra satellite, in particular the ASTER sensor, high spatial resolution data (nominal 15m pixels) is available for purchase. Although not as cost effective as Landsat ETM+, ASTER includes an extra aft-looking infrared sensor that is designed to collect stereo satellite imagery. The ground receiving station then processes this data creating a relative or absolute DEM (30m resolution) to order. Not only will ASTER provide

virtually global coverage, but, as it is polar-orbiting stereo data will be continually collected.

DEM data will clearly be a valuable resource for future glacial landform mapping, whilst placing new demands upon researchers in its use. This chapter has demonstrated that, for landform mapping, they can be superior to satellite imagery. Chapter 6 goes on to explore how best they may be visualised so that they can be utilised in a broad mapping programme. This is illustrated through the application of the techniques developed, to a case study. However the partial global coverage of SRTM and the currently small archives of ASTER means that the continued use of satellite imagery will be necessary.

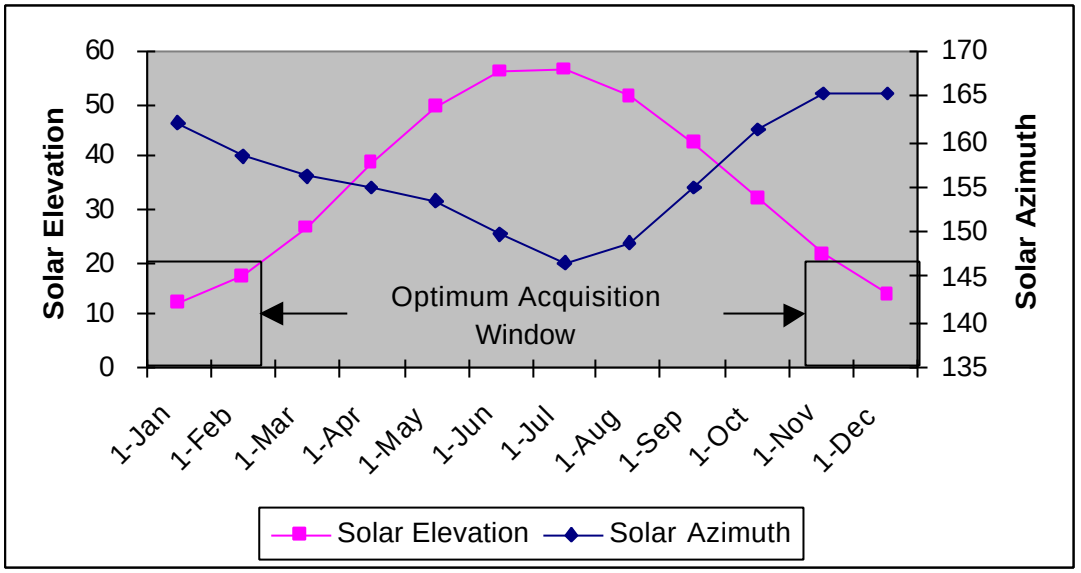

Figure 5.34 Illustration of the variation in solar elevation and azimuth for the Landsat ETM+ scene of Ireland (WRS 207.23). Note the rise in solar elevation from ~10º to ~60º, whilst solar azimuth varies from ~145º to ~165º.